MODIFICATION OF DESIGN CHARACTERISTICS OF X-52 STEEL

BY CHANGES OF FABRICATION PROCEDURES

A THESIS

Presented to

The Faculty of the Graduate Division

by

Yar Mohammad Ebadi

In Partial Fulfillment

of the Requirements for the Degree

Master of Science in Mechanical Engineering

Georgia Institute of Technology

June, 1970

In presenting the dissertation as a partial fulfillment of the requirements for an advanced degree from the Georgia Institute of Technology, I agree that the Library of the Institute shall make it available for inspection and circulation in accordance with its regulations governing materials of this type. I agree that permission to copy from, or to publish from, this dissertation may be granted by the professor under whose direction it was written, or, in his absence, by the Dean of the Graduate Division when such copying or publication is solely for scholarly purposes and does not involve potential financial gain. It is understood that any copying from, or publication of, this dissertation which involves potential financial gain will not be allowed without written permission.

7/25/68

MODIFICATION OF DESIGN CHARACTERISTICS OF X-52 STEEL

BY CHANGES OF FABRICATION PROCEDURES

Approved:

_____

Chairman

Date approved by Chairman: 6/4/70

ACKNOWLEDGMENTS

This thesis is dedicated to my mother, for without her continued love, encouragement, and patience the accomplishment of this work would have been to no avail.

TABLE OF CONTENTS

LIST OF TABLES

LIST OF TABLES (Continued)

LIST OF ILLUSTRATIONS

LIST OF ILLUSTRATIONS (Continued)

SUMMARY

This thesis was undertaken to determine if there might be a hot working temperature range which would result in an optimum combination of X-52 steel mechanical properties, as compared with those properties resulting from usual very high temperature hot mill practices. X-52 is a single alloy addition high strength low alloy (HSLA) steel representative of the new generation of structural steels. Starting material for the experimental program was in two conditions - production mill finished and 20% cold worked. Nine different rolling temperatures were considered in the fabrication program.

Fabrication in the lower extremities of the single phase austenitic region, just above the A_3 line, was found to produce the preferred combination of properties. Ductile-brittle V-notch Charpy 15 foot-pound transition temperature of the resulting plate was unusually low, while yield strength and ultimate tensile strength were improved, without sacrifices in ductility, as compared with production finished X-52 steel.

For X-52 fabricated in the austenitic range higher fabrication temperatures result in larger ferrite grains, and yield strength varies with grain size in accord with the well known Hall-Petch relationship:

$$\sigma_y = \sigma_i + K_y \, d^{-1/2}$$

Fabrication accomplished in the austenite-ferrite or ferrite-cementite two phase regions results in cold work possibly complicated by strain aging: results are steels with high yield strengths, low ductility, and poor ductile-brittle transition temperatures, characteristics resulting from increased values of the lattice friction stress σ_i. As the fabrication temperature is lowered, ferrite grains show increasing degrees of orientation.

Fabrication at the mentioned optimum temperature produces a very favorable microstructure. Ferrite grain size is small and rather equiaxed. Pearlite patches are small and well distributed through the ferrite matrix. There are no indications of cold work. The desirable properties result from strain hardening of the austenite immediately before the austenite-ferrite transformation.

CHAPTER I

INTRODUCTION

Statement of the Problem

Structural steels in many common forms, as plate, sheet, rod, wide flange beams, I beams, channels, pipe, etc. are usually fabricated at the steel mill by hot rolling at temperatures well within the single phase austenitic region, with temperatures within the range of 1700 to 2100°F most often being applicable. Steels of the mentioned type are seldom if ever subjected to hardening heat treatments, as quenching and tempering, but are usually used in the as-hot-rolled condition. Steels of a given composition from given processes (basic oxygen furnace, basic open hearth furnace, etc.; rimmed, killed, semikilled, etc.) will then be represented by a given set of mechanical properties which show but little variation from heat to heat.

The properties considered by the design engineer, at the design and materials selection stage, may include yield strength, ultimate tensile strength, uniform elongation, percent reduction of area, percent elongation, strain hardening exponent, strength coeffi-cient, and the ductile-brittle transition temperature as determined by Charpy impact tests. It is entirely possible that an optimum combination of mechanical properties for a particular design applica-tion may not result from hot rolling in the indicated temperature

range, but may result from fabrication accomplished at other temperatures. This thesis was primarily undertaken in order to investigate these possibilities.

For this thesis the utilized steel was one designated as X-52 as provided and fabricated by the Republic Steel Corporation. X-52 is essentially a plain carbon steel. As an integral part of the thesis samples in two different initial conditions (mill finished and cold worked) were to be fabricated at several temperatures within the single phase austenitic region (above the A_3 line), at temperatures within the critical region (two phase austenite-ferrite range), and at several temperatures within the two phase ferrite-cementite range, below the eutectoid temperature. The temperatures and reductions to be used in the experimental fabrication program were to be based on a combination of experience and theory, and were selected by the author and his advisor with the understanding that they be compatible with limitations of Republic Steel research fabrication facilities. Tensile and Charpy characteristics were to be determined for each of the rolled samples, and the effects of changes of fabrication variables on microstructure were to be investigated by the use of available means.

X-52 Steel

X-52 is a name or designation utilized by the Republic Steel Corporation to indicate one of their proprietary grades of structural steel. The number included in the name (52, in this case) represents the guaranteed minimum yield strength in the units of kips per square

inch (ksi). Although X-52 is essentially a plain carbon steel, some minimal alloy additions have been made or traces are present, and it is usually considered to be a member of the high strength, low alloy (HSLA) grades, and has been so included along with a number of other Republic steel products in a recent data sheet [1].* Properties are enhanced by the utilization of proprietary controlled rolling programs compatible with production facilities.

HSLA steels were developed to provide improved properties and possible cost savings as compared with the utilization of plain carbon steels. Minimum guaranteed yield strengths range from 35,000 to 80,000 psi, depending on the grade considered, which is up to 225% of that for structural plain carbon steels. As compared with the utilization of structural carbon steels there will usually be a 10 to 30% cost savings for equal strength levels, and a 20 to 50% savings in weight based on equal strength. In general, HSLA steels are formable, weldable, machinable, tough, and available in a wide selection of shapes and sizes that can be provided with special properties or characteristics, if required.

Carbon is the primary strengthener, the action being due to the formation of carbides. In order to insure good toughness, weldability, and formability, the carbon content is held as low as possible consistent with strength requirements. Manganese additions promote high strength, improved resistance to abrasion and fatigue, and contribute to toughness. Most HSLA steels have manganese present in

*Numbers in brackets refer to references listed in the Bibliography.

higher concentrations than would be found in the structural plain carbon steels. Copper, Molybdenum, nickel, and chromium are present in X-52, but at the levels involved must be considered as traces or impurities rather than alloy additions.

X-52, and modifications thereof, is available as hot rolled, cold rolled, and galvanized sheet; hot rolled and cold rolled strip; hot rolled plate; hot rolled bars and bar shapes; and hot rolled structural shapes. In addition to the standard hot and cold rolled finishes, some sheet and strip is also available as hot dipped and electrogalvanized, with or without specially prepared surfaces for better paint adherence.

All of the X-52 steel samples provided and fabricated by the Republic Steel Corporation were taken from one 3/8 inch thick plate from heat number 441708 X-52 which had been fabricated in Gadsden, Alabama, facilities by a proprietary, commercial, hot rolling schedule. The chemical analysis included 0.21 C, 1.06 Mn, 0.013 P, 0.015 S, 0.037 Si, 0.05 Cu, 0.04 Ni, 0.03 Cr, 0.014 Sn, and 0.017 Mo, all concentrations being on a weight percent (w/o) basis. As the composition indicates, the steel is essentially a plain carbon steel, with traces of several other elements being present. The manganese content is somewhat higher than would be found with a plain carbon 1020 steel (0.3 to 0.5 w/o C).

Background

Dependence of Properties on Microstructure

If samples of a given metal or alloy are in identical conditions, except for grain size, it is then found that variations of

grain size introduce noticeable and measurable effects on many of the mechanical properties. For example, it has been found at room temperature that hardness, yield strength, ultimate tensile strength, fatigue strength, and impact resistance all increase with decreasing grain size. The effect of grain size is no doubt a maximum when influencing those properties which are related to the early stages of plastic deformation, for it is at these early stages of flow that grain boundary barriers to dislocation motion are most effective. Thus, yield strength would be expected to be more dependent on grain size than would ultimate tensile strength. For the later stages of deformation the flow stress would be controlled chiefly by complex dislocation interactions occurring within the grains, and then grain size would not necessarily be the controlling variable.

A well respected and often utilized relationship between yield strength, σ_y, and grain size (the grain diameter d) is one derived from considerations of basic dislocation theory by Hall [2] and Petch [3], and commonly referred to as the Hall-Petch relationship or equation:

$$\sigma_y = \sigma_i + K_y d^{-1/2} \tag{1}$$

A plot of the variables in this relationship would obviously be linear if yield strength, σ_y, would be put as the ordinate against reciprocal square root grain diameter d as the abscissa. σ_i is considered to be a friction stress which opposes the motion of dislocations, and K_y is a measure of the extent to which the dislocations are piled-up at a barrier, as against a grain boundary. The slope

of the mentioned plot would be used to evaluate K_y, which has been found to be essentially independent of temperature. The intercept σ_i is a measure of the stress required to drive a dislocation against the resistance of impurities, precipitate particles, subgrain boundaries, the inherent Peierls-Nabarro force, and any other obstacles to dislocation motion. The value of the friction stress term depends on composition, condition, and temperature. The Peierls-Nabarro force is temperature dependent, and the other resistances to dislocation motion are influenced by both temperature and composition, indicating the necessity of applying Equation (1) only for a given metal or alloy in identical conditions except for grain size. The Hall-Petch relationship was first proposed for specific cases dealing with low carbon steels, but it has now been applied to a wide variety of steels and nonferrous metals. A recent article, with a partial literature survey, has estimated that the Hall-Petch relationship has now been verified for over 60 cases. Of course, values of σ_i and K_y vary from alloy to alloy, and from condition to condition for a specific alloy.

At this point it is appropriate to consider the various metallurgical phenomena that will influence the value of σ_i when dealing with low carbon steels, and the effects that variations in σ_i values will have on mechanical properties. Many investigators, as for example Pickering and Gladman [4], have considered for the case of plain carbon steels with carbon contents below 0.2 w/o that the value of σ_y is independent of the amount of pearlite in the steel, but that there would be a ferrite grain size effect as indicated by

the Hall-Petch relationship. Thus, it has been possible to develop modified Hall-Petch equations in terms of chemical composition and grain diameter, as will be discussed in later portions of this thesis for annealed, normalized, or hot worked low carbon steels. These research workers have reasoned that although the pearlite patches are very hard, as compared with the ferrite grains, the pearlite patches are so widely dispersed that the ferrite matrix can deform around ferrite grains with but little difficulty. It has been found [5], however, that ferrite grain size generally decreases with increasing pearlite content because the formation of pearlite patches during the austenitic decomposition transformation interferes with ferrite grain growth: consequently, pearlite can indirectly raise the value of yield strength σ_y by raising the value of $d^{-1/2}$ for the ferrite grains. After plastic flow has been initiated in a tensile test and the cross-sectional area of the specimen is reduced, the pearlite patches are then closer together and can exert a possibly significant plastic constraint upon further deformation of the ferrite: a result will be an increase of strain hardening rate, and thus an expected result would be that the ultimate tensile strength of annealed or normalized low carbon steels would be increased by the presence of pearlite to a much greater extent than would the yield strength σ_y [4,5].

It is an established fact that increasing carbon content increases the yield strength of carbon steels [6]. The increase of yield strength occurs because increasing carbon lowers the austenite-ferrite transformation temperature and consequently causes a reduction

in ferrite grain size and also because the friction stress σ_i increases [7] with increasing amounts of dissolved carbon. Both effects are more pronounced as the cooling rate from the austenitic region is increased because the carbon then precipitates at a lower temperature and the grain refining action and precipitation hardening effects are increased.

Small carbon additions to iron also increase the V-notch Charpy ductile-brittle transition temperature [6]. A small fraction of this increase is the result of relatively small increases in the values of the friction stress σ_i, but the principal effect is due to the increasing size and number of carbides that form at ferrite grain boundaries, for a given cooling rate after austenitizing. The increase of carbide facilitates microcrack nucleation leading to brittle fracture.

The V-notch Charpy properties of water quenched steels are generally superior to those of annealed or normalized steels because the fast cooling rate prevents the formation of grain boundary cementite and also results in a refinement of ferrite grain size. However, the grain size of normalized steel can also be refined by lowering the normalizing temperature: the transition temperature of a low carbon steel has been lowered by 125°F by lowering the normalizing temperature from 2200°F to 1650°F [8]. Many commercial grades of steel are utilized in the hot rolled condition and the rolling procedures have a considerable effect on Charpy impact properties. It has been found that rolling to a lower finishing temperature [9,10,11] can lower the impact transition temperature, possibly due to the increased cooling

rate and the correspondingly reduced ferrite grain size. Since
thick plates cool more slowly than thin ones, due to heat transfer
considerations, thick plates will have a larger ferrite grain size
and hence are more "brittle" than thin ones after the same thermo-
mechanical treatment [12]. Post rolling normalizing treatments are
often given to improve the properties of rolled plate [13], for the
just discussed reasons.

Plastic deformation will raise the value of the friction
stress σ_i by strain hardening, and it is well known that the effect
may be unusually large: for example, it is not uncommon for the yield
strength (flow stress) of steels to be doubled or tripled or increased
even further by cold work. The Charpy impact transition temperature
is also raised by cold work: an increase of about $4.5^\circ F$ in the 25%
fibrous fracture appearance transition temperature has been found to
correspond to a 1,000 psi increase in σ_i due to 2% plastic strain [14].

In addition to the effects directly introduced by plastic
deformation or cold work, subsequent aging can also produce addi-
tional increases in the values of σ_i, the actual magnitude of these
increases being dependent on the composition of the steel, aging time,
and aging temperature. The changes of friction stress σ_i are believed
to result from dispersion hardening effects [15] produced by the pre-
cipitation of iron nitride from ferrite solid solution. The return of
the upper yield point on complete aging is thought to result from the
pinning of dislocations by free nitrogen atoms. The increase of fric-
tion stress σ_i due to strain aging promotes strain age embrittlement
[16,17,18], and there is an increase of ductile-brittle transition

temperature of about 3.6°F per 1,000 psi increase in σ_y after aging.
Common steel alloy additions as manganese, aluminum, and vanadium
lower the tendencies toward strain aging embrittlement, the former by
retarding the precipitation of nitrides, the latter two by combining
with nitrogen to form AlN and VN during normalizing and hot rolling.
Silicon is also beneficial in this respect because it is an effective
deoxidizer and leaves the aluminum free to getter the nitrogen.

The referenced literature has indicated that the strongest
influence on the friction stress σ_i is associated with plastic defor-
mation (strain hardening, cold work) and possible subsequent aging.
In regard to plastic deformation, the common or engineering stress-
strain curve is actually no more than a load-elongation curve, and
is not suitable for describing the plastic properties and work harden-
ing characteristics of metals and alloys. It is generally considered
that the true stress - true strain tensile curve can be described by
the empirical relationship:

$$\bar{\sigma} = K \bar{\varepsilon}^n \qquad (2)$$

The equation implies a linear relationship between $\log \bar{\sigma}$ and $\log \bar{\varepsilon}$,
with the slope being the value of the strain hardening exponent n,
and the intercept being the value of true stress at a true strain
value of one, the latter being known as the strength coefficient K.
If a material obeys the relationship expressed by Equation (2), then
Considere's constructions show that it is necessary for the true
strain at the instant of necking to have a value equal to n. The
strain hardening exponent is, then, a measure of the rate of work

hardening of the material being considered. A low value of the slope of the log $\bar{\sigma}$ - log $\bar{\epsilon}$ plot indicates a low rate of work hardening (change of flow stress with change of plastic strain) while a high slope value corresponds to rapid work hardening. Many experimentally determined plots of log $\bar{\sigma}$ against log $\bar{\epsilon}$ do not show complete linearity in the plastic range. Thus, a number of modifications of Equation (2) have been proposed, and a very recent one due to Gladman, Holmes, and Pickering [19] was found to give excellent agreement with experimental data for a number of steels:

$$\bar{\sigma} = a + b \ln \bar{\epsilon} + c \bar{\epsilon} \qquad (3)$$

By optical metallographic techniques it is a relatively simple matter to evaluate some of the variables which may be expected to influence mechanical properties: for example, quantitative metallography will allow an evaluation of ferrite grain diameter d which is one of the variables to appear in the Hall-Petch relationship given by Equation (1). However, optical metallographic techniques do not allow quantitative evaluations of work hardening and strain aging effects; such effects can be treated by electron microscope techniques, by the transmission of the electron beam through thin samples, but such work was beyond the scope of this thesis, partially due to the unavailability of pertinent equipment (an electron microscope).

Many of the alloy additions made to low carbon steels produce some solid solution strengthening of ferrite at ambient temperatures and thereby raise values of the lattice friction stress σ_i. At the same time, these alloy additions may result in the austenite-ferrite

transformation being at lower temperatures, thus producing a refinement in ferrite grain size. Both of these effects will raise the yield strength of such steels in accord with Equation (1). When effects of the type mentioned in this paragraph are the only ones of importance, quantitative metallographic techniques and computer multiple regression analyses of experimental tensile data have allowed the two simple effects to be separated, and it is then possible to express the Hall-Petch relationship in terms of chemical composition, as:

$$\sigma_y = c_1 + c_2 d^{-1/2} + \sum_{i=1}^{N} \alpha_i \qquad (4)$$

α_i is the strength increase in psi per weight percent of alloy addition dissolved in the ferrite. The summation is taken over N alloy additions dissolved in the ferrite. Note that relationships of the type of Equation (4) take no account of cold work, precipitation effects, or other complicated metallurgical phenomena which would be expected to influence strongly values of the friction stress σ_i: this fact can not be overemphasized, and must be kept in mind in the remaining portions of this thesis.

Pioneer work involved with the development of modified Hall-Petch relationships of the type generally designated by Equation (4) was the result of analyses performed by Pickering's group [4,20] at the United Steel Companies, Ltd., of Great Britain. The analyses included variables as grain size and volume fraction of pearlite and effects due to steel alloy additions as manganese and silicon. The analyses were made over a wide range of steel compositions of the

types used for structural applications, and only considered the steels
when in common conditions as would result from normalizing. A result
of the analyses included the formulation:

$$\sigma_y \text{ (psi)} = 15,000 + 4,720(w/oMn) + 12,150(w/oSi) + 507d^{-1/2} \quad (5)$$

Not included in Equation (5) are effects introduced by those alloy
additions which result in more complicated metallurgical phenomena,
as precipitation hardening due to VN or VC, cold work, or strain
aging: in other words, to repeat, relationships as Equations (4) and
(5) are useful for plain carbon steels in metallurgical simple condi-
tions characterized by softness, as would result from normalizing.
Various modifications of Pickering's initial formulation have been
developed as time has passed and in 1967 Jamieson and Thomas [21]
published the following relationship using experimental data for one
steel which was fabricated by two different practices:

$$\sigma_y = 8,700 + 73,900(w/oC) + 12,200(w/oMn) + 102,200(w/oV) + 278d^{-1/2} \quad (6)$$

Duckworth's [22] formulation for hot rolled carbon steels, with Mn
but without Si, is:

$$\sigma_y = 11,872 + 3,189(w/oMn) + 573d^{-1/2} \quad (7)$$

Finally, Irvine [23] has developed the following minor modification
of the Pickering equation by utilizing a larger number of test
results in his computer program, and by considering the influence
of free nitrogen, N_f:

$$\sigma_y = 10,080 + 4,704(w/oMn) + 12,096(w/oSi) + 51,520(w/oN_f^{1/2}) \quad (8)$$

$$+ 502d^{-1/2}$$

Some investigators have found that the effect of pearlite on yield strength may be of more importance than the previous simple reasoning would lead one to believe. Thus, the multiple regression analysis due to Korchynsky [24] and his associates at the Graham Research Laboratories of the Jones and Laughlin Steel Corporation gave further modifications to Pickering's formulation, as follows:

$$\sigma_y = 13,000 + 3,500(w/oMn) + 9,000(w/oSi) + 4,000(w/oNi) \quad (9)$$

$$+ 99(v/o \text{ pearlite}) + 591d^{-1/2}$$

The influence of ferrite grain size and volume fraction of pearlite on the lower yield strength and Luders strain of carbon steels has been further considered in a very recent technical publication by Kouwenhoven [25].

The multiple regression analyses performed by the various investigators with their available data have been extended to include other mechanical properties. As previously mentioned, the ultimate tensile strength would be expected to be influenced by the volume fraction of pearlite present in the microstructure, giving:

$$UTS = 42,700 + 3,990(w/oMn) + 12,000(w/oSi) + 224d^{-1/2} \quad (10)$$

$$+ 560 \ (v/o \text{ pearlite})$$

$$UTS = 32,928 + 3,741(w/oMn) + 378d^{-1/2} + 1,635(v/o \text{ pearlite}) \quad (11)$$

$$\text{UTS} = 19,200 + 18,800(\text{w/oMn}) + 79,700(\text{w/oV}) + 110,000(\text{w/oC}) \quad (12)$$
$$+ 159d^{-1/2}$$

Equation (10) is the result of the older, pioneer, work done by Pickering and his group [4,20]. Equation (11) is analogous to Equation (7), having appeared in the same Duckworth [22] paper, Equation (12) is that of Jamieson and Thomas [21] which treated only one vanadium containing steel fabricated by two procedures.

Only one literature reference [26] could be found which considered the strain hardening exponent n as a function of grain size and (possibly) composition, and the relationship which was developed was an approximation for steels which were metallurgically very simple and were in soft conditions:

$$n = \frac{5}{10 + d^{-1/2}} \quad (13)$$

Since Pickering [4,20] had a great deal of available data and computer time, he also performed regression analyses which gave much wider confidence limits when considering a measure of ductility, percent reduction of area, and also the impact transition temperature. Pickering emphasized that the formulations are not applicable when precipitation hardening effects or cold work are present:

$$\%\text{RA} = 78.5 + 5.39(\text{w/oMn}) - 0.53(\text{v/o pearlite}) - 8,399d \quad (14)$$

$$\text{ITT (}^\circ\text{C)} = 63 + 44.1(\text{w/oSi}) - 228(\text{w/oAl}) + 2.2(\text{w/o pearlite}) \quad (15)$$
$$- 2.3d^{-1/2}$$

As previously pointed out, Equations (4) through (15) were generally developed for metallurgically simple steels, as normalized plain carbon steels, and do not account for complications as would be introduced by precipitation, strain hardening, and strain aging.

Controlled Rolling

The possibility of activating strengthening mechanisms while simultaneously accomplishing hot or warm fabrication has been greatly investigated in recent years, particularly since 1965. Much of the pioneer work was done in the Soviet Union, and British investigators have also been quite active. In some instances controls are exercised immediately after hot or warm fabrication. Some of the research and development experience has been reduced to commercial practice, and is now being utilized in the steel industry with certain alloys. The various procedures are sometimes referred to as "controlled rolling" but are sometimes designated as "thermomechanical treatments," and various classifications have been made:

    a. Isoforming.

    b. Preliminary thermomechanical treatment (PTMT).

    c. High temperature thermomechanical treatment (HTTMT).

    d. Low temperature thermomechanical treatment (LTTMT).

    e. Combined thermomechanical treatment (CTMT).

    f. Controlled cooling and coiling.

"Isoforming" is the designation given to fabrication done simultaneous with the austenite-pearlite reaction. If proper control is exercised, one result will be the obtaining of a fine subgrain structure in the ferrite accompanied by partial spheroidization [27].

Although there were only small improvements in yield and ultimate tensile strengths due to isoforming, there were considerable changes in the ductile-brittle V-notch Charpy transition temperature, resulting in greatly improved toughness.

Concerning results obtained by isoforming, this paragraph will deal with the work of Irani [28]. He concluded that changes of the mechanical property values resulting from isoforming were related to microstructural changes, the most important of which was the formation of subgrain boundaries in the ferrite matrix. Isoforming at 600°C was found to produce the minimum ductile-brittle transition temperature with the particular steels which were investigated. A comparison of the isoformed microstructure with the microstructure resulting from normal hot mill practice showed that:

a. The morphology of the carbide phase was completely altered.

b. The carbide phase in the isoformed steel was rather uniformly dispersed throughout the structure.

c. The ferrite matrix of the isoformed steel was subdivided into subgrains which were equiaxed with a mean diameter of about 0.3 μ.

Irani found that at least 70% reduction was required during isoforming in order to achieve significant lowering of the ductile-brittle transition temperature. Irani's conclusions may be summarized as:

a. The isoforming treatment is very beneficial to the mechanical properties of suitable steels. A slight improvement in values of measures of strength is accom-

panied by marked improvements in impact properties.

b. Compared with bainitic and martensitic structures tem-
    pered to equivalent strength levels, the isoformed steels
    possess significantly superior impact properties.

c. The improvement of mechanical properties due to iso-
    forming are accompanied by three microstructural changes,
    as previously noted.

d. An increase of dislocation density in the matrix ferrite
    increases strength at the expense of impact toughness.

e. An increase of isoforming temperatures above 600°C
    increases subgrain and precipitate particle sizes which,
    in turn, decrease the strength and impact toughness of
    the material.

f. Any low alloy steel with a suitable T-T-T diagram may be
    isoformed.

g. Improved results are obtained when deformation is initiated
    before initiation of the austenite-pearlite reaction, and
    if the transformation is completed during the isoforming
    operation.

Involved with preliminary thermomechanical treatments (PTMT) is
plastic deformation accomplished before austenitization. There are
strengthening effects if the cold work is done before austenitization
and if the cold worked steel is then rapidly heated to the austenite
range. It appears that under properly controlled conditions that at
least some of the dislocations introduced by prior cold work are
retained after the thermal treatment.

During high temperature thermomechanical treatments (HTTMT)
strain hardening is accomplished simultaneously with recrystallization,
even if the fabrication is hot and is done in the stable austenitic
range. Resulting from the operations will be increases in values of
yield strength, ultimate tensile strength, ductility, and fatigue
properties, as compared with values of properties resulting from more
conventional processing. Ivanova and Gordienko [30] have described a
particularly effective HTTMT: steel was heated to the temperature range
of 1150 to 1200°C, thus well within the austenitic region, was then
cooled to a temperature slightly above the A_{c3} line, and was then given
25-30% reduction by rolling at the latter temperature. After the des-
cribed HTTMT treatment the steel was rapidly water quenched and
tempered at 100-200°C. Yield strength increases were of the order of
10% as compared with values obtained from samples of the same steel
given identical thermal treatments without the accompanying plastic
deformation due to rolling. A very fine microstructure was observed
with the HTTMT steel. Deformation at a temperature just above the A_3
line, instead at conventionally higher temperatures, retards the rate
of recrystallization of austenite. Quenching was done to prevent
recrystallization after fabrication. Koppenaal [31] in his recent,
excellent survey of thermomechanical treatments utilized in the Soviet
Union, has concluded that carbides may form during HTTMT when pre-
cipitation hardenable steels are fabricated. The solid solubility of
carbon in austenite was thought to be greatly reduced by the effects
of plastic deformation. However, the carbides would go in to solid
solution as soon as the deformation was completed unless the steel was

quenched. Unfortunately, it is impossible to completely prevent the occurrence of some recrystallization during HTTMT: thus, steels with slow recrystallization kinetics, as tool and heavily alloyed engineering steels, are considered to be particularly applicable for HTTMT [32].

The process designated as low temperature thermomechanical treatment (LTTMT) are also known as "ausforming," and the technical literature dealing with ausforming is rather extensive since old principles are involved. To be applicable, LTTMT must be done with a steel capable of forming martensite: processing consists of fabrication at a temperature below the recrystallization range but above the martensite start M_s temperature. A typical LTTMT is described in the Russian booklet translation [30], and the amount of deformation given was 75 to 90% reduction by rolling. LTTMT can result in very high increases in yield strength and usually results in increased ductility, as compared with results obtained with HTTMT of the same steel, but there have been cases where ductility decreases were noted. High alloy steels are very suitable for LTTMT since there is a sufficiently wide metastable austenite bay in the T-T-T diagram for these steels to allow sufficient time for fabrication to be accomplished. LTTMT may produce a number of microstructural changes. Since the deformation temperature is below the solution temperature for many of the carbides, simultaneous deformation and carbide precipitation may result. Another important feature of LTTMT is that during the austenite-martensite transformation the high dislocation density of the deformed austenite is retained by the martensite, resulting in increased resistance to

plastic deformation in the final product.

Combined thermomechanical treatment (CTMT) involves a combination of HTTMT and LTTMT in one fabrication program. Encouraging results [31] have been obtained with medium carbon steels (0.30 - 0.40 w/o C) containing tungsten, vanadium, nickel, and/or molybdenum additions. Yield strength increases of 35 to 45% and ultimate tensile strength increases of 10 to 30% have resulted from application of CTMT, the values of yield and ultimate tensile strength being compared with those resulting from conventional hot rolling.

For the cases involving relatively thin strip and sheet products, where the heat transfer characteristics are not overwhelming as they would be with thick plate, the combination of accelerated cooling just after leaving the hot mill and controlled coiling temperatures has received research and development attention. Cryderman, Coldren, Bell, and Grozier [33] investigated the influence of various cooling schedules on quarter-inch plate of various structural steels modified with boron, molybdenum, and columbium. Strength increases resulting from the experimental program were attributed to refinement of ferrite grain size. Previously completed investigations [34] had resulted in the conclusion that accelerated cooling did not effectively suppress the recrystallization of austenite in carbon steels, although there was such a suppression when dealing with precipitation hardenable steels. Controlled cooling of steel strip or sheet after coiling can also play an important part in property control. If the austenite decomposition transformation has not been completed prior to coiling,

when the steel is still on the run-out table, then the transformation
will continue in the coil and precipitation hardening may take place
in those steels which are vanadium and columbium containing.

CHAPTER II

MATERIAL AND SPECIMEN PREPARATION

The Fabrication Program

The X-52 steel utilized in this program was taken from one piece of 3/8 inch thick plate processed and fabricated by the Republic Steel Corporation in their production facilities in Gadsden, Alabama. The steel was commercial in every sense of the word, having been a part of a production run. The rolling procedures which were used in Gadsden were proprietary, and hence were not revealed to the writer of this thesis; however, it is understood that some exercise of controlled rolling was involved, the practice being consistent with production scheduling. The composition and heat number for the steel samples which were supplied by Republic Steel Corporation have been previously mentioned in this thesis.

The controlled rolling program which was formulated was intended to cover as many of the various thermomechanical treatments as were thought to be applicable to the particular steel being worked with. Low temperature mechanical treatment (LTTMT) was an impossibility: the T-T-T transformation diagram for X-52 is not of a type appropriate for LTTMT since metastable austenite decomposition at temperatures below the A_1 will be initiated in very short times, much shorter times than those required to bring 3/8 inch thick plate to desired fabrication temperatures. Since LTTMT could not be investigated, there was

then the additional result that combined thermomechanical treatment (CTMT) could not be dealt with. The programs which were eventually developed had to be consistent with the limitations and capabilities of the facilities of the Republic Steel Research Center, where the experimental fabrication was accomplished, and also had to be consistent with the sizes of samples which were available for fabrication. Thus, the controlled cooling and coiling processing variables could not be investigated, since no coiling facilities were available on the research rolling mill, and since coiling would have been completely impractical for the available specimen sizes.

The controlled rolling program which was developed was able to include several thermomechanical treatment possibilities, and was sufficiently appealing to Republic Steel personnel to warrant the time and expense necessary on their part to carry out the fabrication. Included in the thermomechanical treatment possibilities covered by the experimental fabrication were: (a) high temperature thermomechanical treatment (HTTMT), at temperatures sufficiently high in the austenite range that all carbides should be in solution, at temperatures at which carbide precipitation would be concurrent with fabrication, and at temperatures actually below the A_3 line; (b) isoforming, the various temperatures being selected so that the austenite decomposition takes place simultaneously with deformation, and (c) preliminary thermomechanical treatment (PTMT) since half of the plate samples were cold worked before being hot or warm worked at the rolling mill. Included in the experimental rolling program were rolling temperatures which may be considered as unusually low, even for

thermomechanical treatments. Selected fabrication temperature ranges
extended well below the A_1 line, thus allowing a further investigation
of effects introduced by cold work and possible simultaneous aging.

From the previously mentioned 3/8 inch thick X-52 plate a
total of 20 plate samples were prepared for utilization in the exper-
imental fabrication program. One of the twenty samples was set aside
without further processing, was given the designation "A," and was
considered to be representative of the mill produced steel, as rolled
in production facilities in Gadsden. For all cases the plate sample
size was ten inch length by six inch width by plate thickness, and
the length direction was in the rolling direction of the initial 3/8
inch plate and was also in the rolling direction for all subsequent
experimental fabrication. The mentioned plate sample size (10" x 6"
x 3/8") was dictated by the capacity of available furnaces adjacent
to the rolling mill at the Republic Steel Research Center and by the
capabilities of the rolling mill itself. The rolling mill was of the
two-high configuration, was reversing, had 14 inch diameter rolls of
20 inch effective length, and was operated at 1,000 rpm during all
controlled rolling experimentation.

Ten of the plate samples were given an initial 20% reduction of
thickness, to 0.30 inch, by cold rolling at room temperature. These
ten samples were then the ones to be utilized in the preliminary
thermomechanical treatment (PTMT) part of the program. One of the
cold rolled plate samples was designated as "B" and was set aside,
without further processing, to be representative of cold worked X-52.
The remaining nine cold worked samples were each introduced into a

furnace at a high temperature (2000, 1850, 1700, 1550, 1400, 1250, 1100, 940, and 850°F), were allowed to remain in the furnace for one hour, and were then removed from the furnace and as rapidly as possible reduced another 20% in thickness, to 0.24 inch, by one pass through the rolling mill. The nine samples here considered then received two treatments consisting of a 20% initial cold reduction followed by a 20% reduction at each of nine temperatures. These nine samples will hereafter be referred to as the "cold worked - hot worked" materials, and the designation of such samples is indicated by Table 1.

Table 1. Code or Designation of "Cold Worked - Hot Worked" Steels

Furnace Temperature, °F	Code or Designation
800	C
950	D
1100	E
1250	F
1400	G
1550	H
1700	I
1850	J
2000	K

The nine remaining plate samples, each in the mill produced condition and each with a thickness of 3/8 inch, were introduced into a furnace at high temperature (the same temperatures as mentioned in the last paragraph), were held in the furnace for one hour, and were then as rapidly as possible rolled to 0.24 inch thickness in two mill passes of 20% reduction each. There was only an elapsed time of a

very few seconds between each of the two mill passes, and thus there was little opportunity for the plate samples to change temperature by cooling. The nine samples described in this paragraph will hereafter be referred to as "Isothermal" materials, and the code or designation of each sample is indicated by Table 2.

Table 2. Code or Designation of "Isothermal" Steels

Furnace Temperature, °F	Code or Designation
800	L
950	M
1100	N
1250	O
1400	P
1550	R
1700	S
1850	T
2000	V

In addition to the codes or designations indicated by Tables 1 and 2, it must be remembered that "A" designated X-52 in the mill condition, and "B" designated mill condition X-52 given 20% cold work by rolling at room temperature.

Although controlled cooling and coiling could not be investigated as a thermomechanical processing variable, as previously discussed, efforts were made to insure that each sample fabricated at the Republic Steel Research Center did receive rather equivalent cooling, so as not to introduce uncontrolled variables. Each sample was placed in a granular material specifically provided for cooling purposes immediately after exiting from the rolling mill.

Machining of Mechanical Test Specimens

Tensile Specimens

The machining of all test specimens, be they tensile, Charpy, hardness, or metallographic, was done by various procedures accomplished in the Machine Shop Laboratory of the School of Mechanical Engineering at the Georgia Institute of Technology. Acknowledged machine shop personnel gave guidance and assistance; however, nearly all machining was done by the writer himself. Actually, Mr. Pereyra was simultaneously accomplishing a related thesis requiring similar methods of specimen preparation, and the two of us worked together as a team in both the Machine Shop and Testing Laboratories. Machining operations were carefully and most conservatively done, so as to avoid distortion, heating, or other undesirable effects which would in themself influence mechanical properties.

As an initial operation for the preparation of tensile specimens two longitudinal rolling direction blanks and one transverse blank were saw cut from the fabricated plate samples at locations indicated by Figure 1. If the preparation of additional specimens was found to be necessary, as was the case with some codes or designations, the blanks had equivalent locations. Blanks were approximately 5/8 inch in width. As the next operation the flat blanks were rough turned to half inch diameter on a Monarch Model 12 CK lathe. Ends were threaded over a length of about one inch (1/2 inch diameter, 13 threads per inch) and of course flats remained after threading, the distance between the flats being the thickness of the plate (0.24 inch).

Preliminary experimentation had shown that threaded ends of the indi-
cated size, even with the flats, were sufficient to allow all plastic
deformation to take place in the gage section of the specimens, not in
the threaded ends. The gage section of each tensile test specimen was
machined in a Monarch Model 14C lathe equipped with a True-Trace Model
106 633 tracer attachment. Final dimensions of tensile test specimens
were in accord with ASTM Specification E-8. Gage section diameters
of about 0.20 inch were necessary because of the thinness of the plate
from which the specimens were prepared. Of course, each tensile speci-
men was carefully and precisely measured before testing.

Charpy Specimens

The first operation to be accomplished during the machining of
fabricated plate was the removal of about 3/4 inch of material by a
saw cut made with a power hack-saw. This material, indicated by
Figure 1, was discarded since it was thought that it may not be rep-
resentative of the bulk of the plate due to ends effects possibly
introduced by fabrication and furnace heating. As the next step a 2.2
inch long piece of plate was cut in a single operation of the power
hack-saw: this piece, as indicated by Figure 1 was to be used for
the preparation of V-notch Charpy specimens. The described plate sec-
tion was surface ground to standard Charpy specimen length (55 mm)
with a Blohm-Simplex 5 surface grinder with a 12 inch diameter wheel
of the "all purpose" type. Depth of grind with this surface grinder
was never allowed to exceed 0.005 inch, to prevent heating of the
plate. As added insurance to prevent heating, water cooling was pro-
vided during all grinding operations done with the Blohm-Simplex unit.

While utilizing the same surface grinding unit, the plate sections were also ground to a thickness of 0.197 inch by removing approximately equal amounts of material from each side of the plate. A dimension of 0.197 inch corresponds to half-thickness of a standard Charpy specimen, and this dimension is commonly used in steel mill practice and is in accord with ASTM Specifications. Blanks for the final preparation of Charpy specimens were saw cut from the ground plate sample by utilizing a DoAll Metalmaster band saw with a blade of 1/4 inch depth and 14 teeth per inch. Each Charpy blank was given a number, so as to identify location relative to the plate, and was also stamped on the ends with the appropriate letter designations of Tables 1 and 2. After grinding of the saw cut surfaces to the desired Charpy width of 10 mm, a standard V-notch of two mm depth was machined by the use of a specially prepared cutter mounted in a Milwaukee Model H horizontal milling machine. Final dimensions of the Charpy specimens corresponded to tolerances listed in ASTM Standard E-23.

Hardness Specimens

Rockwell hardness determinations were made on the sides of fractured Charpy specimens. Brinell hardness determinations were made on the material between the longitudinal rolling direction tensile specimens as shown in Figure 1; this material was surface ground before Brinell testing.

Preparation of Metallographic Specimens

The locations of metallographic samples relative to the pieces of fabricated plate are indicated by Figure 1; note that the

metallographic samples are thus adjacent to the tensile specimen locations. All of the metallographic samples were prepared by rather standard procedures commonly used with carbon steels of the same carbon content as X-52. The metallographic samples extended across the thickness of the plate, from top to bottom, were of about one-half inch length in the rolling direction, and were oriented so as to have their planes of polish parallel with the rolling direction. All grinding, polishing, and etching operations were done in the Metallographic Laboratory of the School of Mechanical Engineering, although some re-etching was done in School of Chemical Engineering laboratories when metallographic observations were being made. The Bakelite mounted specimens were ground with AB Carbimet Silicon Carbide papers with grits including 180, 240, 320, 400, and 600. Polishing was done on 8 inch diameter rotating wheels equipped with Buehler AB Microcloth: rough polishing was done with Buehler Alpha Micropolish, 0.3 micron diameter, and final polishing utilized as a grit Buehler Gamma Micropolish, 0.05 micron diameter. Various concentrations of Nital solution, in the range from two percent to five percent, were used for etching, it being found that the preferred contrasts of microstructural features did not always result from the use of the initially utilized three percent Nital solution.

Figure 1. Locations of Specimen Blanks.

CHAPTER III

PROPERTY EVALUATION TECHNIQUES

Hardness Testing

Rockwell determinations of hardness were made with a Wilson Mechanical Instrument Division, American Chain and Cable Company, unit located in the Metallography Laboratory of the School of Mechanical Engineering. As mentioned, Rockwell indentations were made on the sides of fractured Charpy specimens, the previously machined surfaces being ideal for such determinations. No indentations were made near the deformed material adjacent to fracture surfaces, since this material would be work hardened. At least 10 Rockwell hardness determinations were made for each code or designation listed in Tables 1 and 2. The majority of testing was done with the B scale which utilizes a 100 kg major load and a 1/16 inch diameter spherical indentor. In some instances the steel samples were beyond the hardness limit (R_b 100) for the B scale, and in these cases the C scale was used, necessitating a change to the diamond brale with a 150 kg major load.

A Brinell testing unit manufactured by the Steel City Testing Laboratory, Tinius Olsen Testing Machine Company, and located in the Mechanical Engineering Metallography Laboratory, was also used. All determinations were made after applying a load of 3000 kg to a standard 10 mm diameter spherical indentor.

Tensile Testing

All tensile testing was accomplished with the 10,000 pound capacity floor model Instron machine located in Room 108 of the Space Science and Technology 1 Building. All testing was done at room temperature with a crosshead velocity of 0.05 inch per minute. An Instron Model G51-12 extensometer was used for determinations of elongation.

Our Model TTC Instron machine is well instrumented, and load-elongation diagrams were autographically recorded on ten inch wide chart paper. The Instron machine was operated at either 10,000 pound or 5,000 pound capacity, depending on the code designation of steel being tested, while the extensometer was correspondingly set for either 25% or 50% maximum elongation. The just mentioned combinations result in load-elongation diagrams of maximum possible size, for the steel conditions being evaluated.

The Instron recorded load-elongation diagrams were analyzed by optically determining values of load at each percent of plastic strain, although for those specimens which were found to be in hardened conditions and which thus gave but little ductility before fracture, load values were determined at each half percent of plastic strain. Values of load were converted to values of engineering stress, and the resulting stress-strain data was tabulated in columnar form. True stress and true strain values were then calculated by application of conversion formulations applicable to that portion of the stress-strain curve obtained before necking commences:

$$\bar{\sigma} = \sigma \, (1 + \varepsilon) \tag{16}$$

$$\bar{\varepsilon} = \ln \, (1 + \varepsilon) \tag{17}$$

Several decisions had to be made before the strain hardening exponent n and strength coefficient K values defined by Equation (2) were calculated. Decisions were required since it was generally found that plots of log $\bar{\sigma}$ as the ordinate against log $\bar{\varepsilon}$ as the abscissa were not exactly linear: these plots were made for each test specimen which was successfully tested. One set of n and K values were calculated by evaluating the slopes of the plotted log $\bar{\sigma}$ - log $\bar{\varepsilon}$ diagrams at the maximum load, as indicated by the strip-chart record, to give n values, and by then using these n values and the maximum load values with Equation (2) to calculate K values. Another set of n and K values were obtained by using Considere's finding that the true uniform elongation has a value equal to n, and then by using these values of n with maximum load values to calculate K values from Equation (2). The two sets of n and K values so calculated generally showed but little deviation.

Other results obtained from direct use of the load-elongation records included upper yield point and lower yield point values, when applicable, or 0.2% offset yield strength. The uniform elongation was measured from the recorded chart, as was the total elongation to fracture. Specimen diameters at the fractures were measured, and percent reduction of area values were then calculated, to give other measures of ductility besides total elongation. Values of engineering stress at fracture were obtained by dividing the fracture load, as

recorded, by the initial specimen cross-sectional area, while for true fracture stress determinations the actual fracture area was utilized.

As is nearly always the case in an extensive tensile testing program, some of the tensile specimens necked and fractured at the radius at each end of gage lengths, instead of in the gage sections, and for those cases extra tensile specimens were prepared and tested. When it was found that the three tensile specimens for any one code designation gave differences of results, as significantly different values of yield strength, ultimate tensile strength, elongation, etc., then extra specimens were also machined and tested. Thus, the number of actual tensile tests exceeded the minimum of 60 resulting from just three specimens from each of 20 different code designations.

Charpy Impact Testing

All experimental determinations of V-notch Charpy behavior were done with the 220 foot-pound capacity Tinius Olsen Charpy-Izod unit located in a laboratory in the old Engineering Science and Mechanics Building: the laboratory is jointly shared by Engineering Science and Mechanics and Mechanical Engineering. The objective was to determine Charpy energy values over the entire transition temperature range, from very brittle behavior to very ductile fracture: thus, the actual temperature ranges to be investigated varied from code designation to code designation.

Controlled variations of test temperature were obtained by using liquid baths in wide-mouthed thermos flasks: specimens were

immersed in the appropriate liquid baths for at least 30 minutes
before being tested. Elapsed time between specimen removal from the
bath and rupturing of the test bar was less than two seconds in all
cases, giving but minimum opportunity for change of temperature from
the bath temperature.

Elevated temperature testing utilized water as the bath.
Temperatures below the ambient were obtained by mixtures or solutions
of ice and water, ice and salt and water, dry ice and acetone, or
liquid nitrogen and ethyl alcohol. Once proper concentrations of mix-
tures or solutions were established, remarkably stable temperatures
were obtained in the thermos flasks. Calibrated thermometers, capable
of being read to at least one degree, were used to measure tempera-
tures of the baths.

Energy values obtained from the 220 Charpy tests were plotted
as the ordinate against the temperatures of testing as the abscissa,
and the 15 foot pound transition temperatures was then determined from
such plots. With X-52 it was impossible to measure fracture appear-
ance transition temperatures, as determined by the ratio or percentage
of fracture surfaces which are ductile.

Quantitative Metallography

During recent years there has been considerable development in
that branch of engineering and science which has become to be known
as "Quantitative Metallography." A number of relationships, as the
Hall-Petch relationship of Equation (1), have been developed relating
microstructural features with mechanical behavior. A more quantitative

treatment of these microstructural features has been desired. Statistical, metric, or numerical means have been used to deduce values of microstructural features in three dimensions from observations made at the microscope or metallograph in two dimensions. Much of the recent work has been summarized in Underwood's new book [35] which primarily deals with the numerical or quantitative characterization of points, lines, surfaces, and volumes.

For this thesis a study of the following items was made for each of the code designations of Tables 1 and 2:

    a.   Volume fraction of pearlite.

    b.   Ferrite grain diameter.

    c.   Pearlite patch diameter.

    d.   Degree of orientation of ferrite grains.

    e.   Degree of orientation of pearlite patches.

In order to allow the study to be made, a minimum of four photomicrographs of each metallographic sample were made with the Vickers Metallograph in the School of Chemical Engineering. Although a number of magnifications were used, the majority of photomicrographs were at either 100, 200, or 400X.

The usual point counting operation was used to determine the volume fraction of pearlite. A grid of 1/4 inch squares was placed over the photomicrograph so as to have one axis of the grid in the rolling direction. The number of intersection points of the grid which lay over pearlite features were counted, and the total number of intersection points was known. The volume fraction of pearlite is simply the ratio of the two mentioned quantities.

The same grid that was used for pearlite determinations, while similarly oriented with respect to photomicrographs, was used to allow calculations of the ferrite grain diameter d: however, the technique was considerably different. In this case it was necessary to count the number of times that a microstructural feature, as grain boundaries, cut grid lines, so that the number of features per unit length of grid line may be calculated. Note that there are several types of "grain boundaries" in steels such as X-52, including ferrite-ferrite, ferrite-pearlite, and pearlite-pearlite. Consider the following formulation and definitions:

$$(P_L)_{\alpha\alpha} = \frac{(P_{\alpha\alpha})_{||} + (P_{\alpha\alpha})_{\perp}}{\text{total length of grid lines}} \tag{18}$$

where: $(P_L)_{\alpha\alpha}$ = number of intersections of ferrite-ferrite grain boundaries with grid lines, per unit length of grid line.

$(P_{\alpha\alpha})_{||}$ = total number of intersections of ferrite-ferrite grain boundaries with rolling direction grid lines.

$(P_{\alpha\alpha})_{\perp}$ = total number of intersections of ferrite-ferrite grain boundaries with transverse grid lines.

Similar to Equation (18), there can be written:

$$(P_L)_{\alpha\beta} = \frac{(P_{\alpha\beta})_{||} + (P_{\alpha\beta})_{\perp}}{\text{total length of grid lines}} \tag{19}$$

The various symbols indicate the same quantities as in Equation (18) except that with Equation (19) it is the ferrite-pearlite grain

boundaries which are considered.

Another important quantity may be defined in terms of the previously discussed terms, as follows:

$$(N_L)_\alpha = \frac{2(P_L)_{\alpha\alpha} + (P_L)_{\alpha\beta}}{2} \qquad (20)$$

where: $(N_L)_\alpha$ = the number of intersections of ferrite grains, per unit length of grid line.

After $(N_L)_\alpha$ has been evaluated by use of the photomicrographs and grid, the ferrite grain diameter d can then be calculated from:

$$d_\alpha = \frac{(1 - \frac{\text{% Pearlite}}{100})}{(N_L)_\alpha} \times \frac{1}{f} \qquad (21)$$

where: f = magnification

After the evaluation of $(P_L)_{\alpha\beta}$ by the utilization of Equation (19), the number of intersections of β(pearlite) grains per unit length of grid line can be found from:

$$(N_L)_\beta = \frac{(P_L)_{\alpha\beta}}{2} \qquad (22)$$

After a value of $(N_L)_\beta$ is obtained from Equation (22), the pearlite patch diameter d can be evaluated from:

$$d_\beta = \frac{\text{% Pearlite}}{100(N_L)_\beta} \times \frac{1}{f} \qquad (23)$$

Twinned metals, banded rocks, and certain dislocation arrays are several of the many examples of oriented structures which occur

in nature. Oriented structures may be divided into two categories:

    a. Completely oriented, or idealized structures.

    b. Partially oriented structures.

Both categories can be described by methods for characterizing the
angular variation of lines or surfaces with respect to an orientation
axis (axes) or orientation plane (planes). A "degree of orientation,"
which is a numerical index, could be used for describing oriented
systems. Since this thesis did not encounter any completely oriented
structures, attention will only be paid to the partially oriented case.
Grains elongated in a particular direction, as the rolling direction,
would be a pertinent example of a partially oriented structure. The
degree of orientation of ferrite grains may be evaluated by use of
the following formulation, and a derivation for this relationship and
a considerable discussion is given in Underwood's textbook [35]:

$$\Omega_\alpha = \frac{(N_L)_{\alpha\perp} - (N_L)_{\alpha\|}}{(N_L)_{\alpha\perp} + 0.571(N_L)_{\alpha\|}} \tag{24}$$

where: Ω_α = degree of orientation of ferrite grains.

    $(N_L)_{\alpha\|}$ = number of intersections of ferrite grains, per unit
                   length of grid line parallel to the orientation axis,
                   and hence in the rolling direction

    $(N_L)_{\alpha\perp}$ = number of intersections of ferrite grains, per unit
                   length of grid line perpendicular to the orientation
                   axis, and hence in the transverse direction.

Similarly, the degree of orientation of pearlite patches may be eval-
uated from:

$$\Omega_\beta = \frac{(N_L)_{\beta\perp} - (N_L)_{\beta\parallel}}{(N_L)_{\beta\perp} + 0.571(N_L)_{\beta\parallel}} \tag{25}$$

where $(N_L)_{\beta\perp}$ and $(N_L)_{\beta\parallel}$ are the number of intersections of β (pearlite) patches per unit length of grid line perpendicular to and parallel with the orientation axis (rolling direction), respectively.

CHAPTER IV

TEST RESULTS

Evaluations of Mechanical Properties

Hardness Tests

Included in Tables 3 and 4 are the Brinell Hardness Numbers obtained by averaging results from three separate determinations for each fabricated sample of X-52. All Brinell testing was done while utilizing the standard combination of 3,000 kg load and 10 mm diameter ball. Also included in Tables 3 and 4 are results obtained by testing with Rockwell units, and both the B scale (100 kg major load, 1/16 inch diameter ball) and C scale (150 kg major load, diamond brale) have been used. Each listed Rockwell hardness value represents the average of 10 individual test results.

Tensile Tests

Tensile test results obtained by calculations performed with data taken from Instron recorded load-elongation curves are summarized in Tables 5 through 16. Tables 5, 6, 7, and 8 have to do with those properties involved with yielding, as upper yield point and lower yield point or 0.2% offset yield strength, yield point drop, and yield point elongation. Included in Tables 9, 10, 11, and 12 are values of those properties primarily associated with necking, including ultimate tensile strength, uniform elongation, strain hardening exponent n, and strength coefficient K. In Chapter III it was pointed out

that the latter two properties, n and K, were each evaluated by two different methods. Tables 13, 14, 15, and 16 are concerned with values of properties associated with fracture, including engineering fracture stress, true fracture stress, percent reduction of area, and percent elongation in one inch.

Charpy Impact Tests

Energy values obtained with each individual Charpy V-notch test specimen are listed in Tables 17 and 18, for "isothermal" and "cold worked - hot worked" specimens, respectively. Values of the 15 foot-pound transition temperature obtained from appropriate construction plots are given in Tables 19 and 20.

Quantitative Metallography Results

Results obtained by individual analyses of the various photomicrographs are listed in Tables 21 and 22. Calculated results include ferrite grain diameter (inches), $d^{-1/2}$ as appearing in the Hall-Petch equation, percent of the microstructure appearing as pearlite, and orientation factor Ω.

Table 3. Hardness Determinations: Isothermal Specimens

Code	Finishing Temperature °F.	Rockwell B	Rockwell C	Brinell, 3000 Kg 10 mm ball
A	Mill	77	--	135
L	800	--	25	262
M	950	--	22	245
N	1100	98	--	222
O	1250	94	--	195
P	1400	89	--	175
R	1550	87	--	165
S	1700	87	--	165
T	1850	86	--	162
V	2000	84	--	155

Table 4. Hardness Determinations: Cold Work - Hot Work Specimens

Code	Finishing Temperature °F	Rockwell B	Rockwell C	Brinell, 3000 Kg 10 mm ball
B	Cold Rolled	94	--	195
C	800	--	24	255
D	950	99	--	230
E	1100	95	--	202
F	1250	86	--	162
G	1400	85	--	158
H	1550	80	--	143
I	1700	88	--	170
J	1850	90	--	179
K	2000	86	--	162

Table 5. Tensile Test Results Related to Yielding; Isothermal, Longitudinal Specimens

Code	Finishing Temperature, °F	Upper Yield Point, psi	Lower Yield Point, psi	0.2% Offset Yield Strength, psi	Yield Point drop, psi	Yield Point Elongation, %
A₁	Mill	50,530	46,480	--	4,050	1.35
A₂	Mill	51,560	46,740	--	4,820	1.35
L₁	800	--	--	117,930	--	0
L₂	800	--	--	119,160	--	0
M₁	950	--	--	111,010	--	0
M₂	950	--	--	95,020	--	0
M₄	950	--	--	103,220	--	0
N₁	1100	--	--	84,890	--	0
N₂	1100	85,940	85,070	--	870	0.35
O₂	1250	75,000	72,710	--	2,290	1.58
O₁	1250	74,050	73,260	--	790	0.85
P₂	1400	67,690	61,610	--	6,080	2.7
P₁	1400	65,660	61,320	--	4,340	3.0
R₁	1550	63,010	58,640	--	4,370	1.9
R₂	1550	55,340	53,460	--	1,880	2.25
R₄	1550	58,630	54,910	--	3,720	1.7
S₁	1700	58,990	58,700	--	290	0.75
S₂	1700	54,520	47,740	--	6,780	1.9
S₄	1700	61,120	55,890	--	5,230	1.4
T₁	1850	57,800	53,460	--	4,340	1.3
T₂	1850	50,240	46,480	--	3,760	1.25
V₁	2000	46,190	45,910	--	280	1.0
V₂	2000	51,830	51,190	--	640	0.9
V₄	2000	51,590	46,050	--	5,540	1.25

Table 6. Tensile Test Results Related to Yielding:
Cold Work—Hot Work, Longitudinal Specimens

Code	Finishing Temperature, °F	Upper Yield Point, psi	Lower Yield Point, psi	0.2% Offset Yield Strength, psi	Yield Point drop, psi	Yield Point Elongation, %
B_1	Cold Rolled	--	--	101,000	--	0
B_2	Cold Rolled	--	--	101,910	--	0
C_1	800	--	--	119,770	--	0
C_2	800	--	--	119,640	--	0
D_1	950	--	--	97,660	--	0
D_2	950	--	--	97,930	--	0
E_1	1100	81,280	79,850	--	1,430	1.1
E_2	1100	80,620	80,010	--	610	1.0
F_1	1250	61,940	59,370	--	2,570	1.6
F_2	1250	60,860	60,000	--	860	1.3
G_1	1400	60,770	58,640	--	2,130	0.8
G_2	1400	59,360	56,750	--	2,610	1.2
H_1	1550	52,990	50,670	--	2,320	1.6
H_2	1550	51,970	51,100	--	870	1.6
I_1	1700	54,720	50,090	--	4,630	0.7
I_2	1700	60,770	58,760	--	2,010	1.0
I_4	1700	52,010	47,750	--	4,260	1.3
J_1	1850	62,020	57,690	--	4,330	1.0
J_2	1850	49,660	47,640	--	2,020	1.0
K_1	2000	--	--	45,850	--	0
K_2	2000	--	--	52,850	--	0
K_4	2000	--	--	45,560	--	0

Table 7. Tensile Test Results Related to Yielding: Isothermal, Transverse Specimens

Code	Finishing Temperature, °F	Upper Yield Point, psi	Lower Yield Point, psi	0.2% Offset Yield Strength, psi	Yield Point drop, psi	Yield Point Elongation %
A_3	Mill	51,500	46,920	--	4,580	1.7
L_3	800	--	--	114,830	--	0
M_3	950	102,100	101,670	--	430	0.9
N_3	1100	87,600	86,810	--	790	1.05
O_3	1250	75,360	73,370	--	1,990	1.28
P_3	1400	66,650	62,690	--	3,960	3.05
R_3	1550	67,590	63,280	--	4,310	1.45
S_3	1700	58,740	54,730	--	4,010	1.4
T_3	1850	53,730	47,700	--	6,030	1.45
V_3	2000	49,250	46,800	--	2,450	1.1

Table 8. Tensile Test Results Related to Yielding: Cold Work - Hot Work, Transverse Specimens

Code	Finishing Temperature, °F	Upper Yield Point, psi	Lower Yield Point, psi	0.2% Offset Yield Strength, psi	Yield Point drop, psi	Yield Point Elongation %
B_3	Cold Rolled	--	--	86,000	--	0
B_5	Cold Rolled	--	--	90,170	--	0
C_3	800	--	--	113,290	--	0
D_3	950	99,410	98,840	--	570	0.5
E_3	1100	79,810	78,670	--	1,140	1.4
F_3	1250	62,990	60,110	--	2,880	1.5
G_3	1400	67,330	60,050	--	7,280	1.5
H_3	1550	52,120	50,690	--	1,430	2.1
I_3	1700	49,030	47,000	--	2,030	0.6
I_5	1700	51,070	46,480	--	4,590	1.5
J_3	1850	--	--	53,190	--	0
K_3	2000	--	--	45,700	--	0
K_5	2000	52,260	49,370	--	2,890	0.8

Table 9. Tensile Test Results Related to Necking: Isothermal, Longitudinal Specimens

Code	Ultimate Tensile Strength, psi	ε_{uts} Uniform Elongation, %	Strain Hardening Exponent, n UTS	Strain Hardening Exponent, n Graph	Strength Coefficient, K UTS psi	Strength Coefficient, K Graph psi
A_1	73,910	19	0.17395	0.1791	119,220	120,300
A_2	73,660	17.9	0.16467	0.1724	116,880	118,500
L_1	122,520	3.0	0.029559	0.035162	140,070	142,800
L_2	123,680	3.0	0.029559	0.033422	141,360	143,260
M_1	120,400	4.6	0.044973	0.05006	144,790	147,050
M_2	103,630	4.5	0.044017	0.068965	124,260	133,520
M_4	112,610	4.3	0.042101	0.067415	134,220	144,480
N_1	96,630	6.6	0.063913	0.062929	122,810	122,470
N_2	96,320	6.6	0.063913	0.074626	122,410	125,960
O_1	85,600	8.8	0.084341	0.084626	114,740	114,810
O_2	85,020	8.2	0.07881	0.077022	112,380	111,880
P_1	78,250	15.6	0.14497	0.14141	119,670	118,860
P_2	78,540	14.2	0.13278	0.1341	114,280	117,580
R_1	81,010	14.2	0.13278	0.13072	120,970	120,450
R_2	75,660	15.7	0.14583	0.14306	115,920	115,300
R_4	79,220	14.2	0.13278	0.12681	118,290	116,850
S_1	83,740	12.5	0.11778	0.1125	121,190	119,820
S_2	72,210	17.6	0.16211	0.16949	114,040	115,570
S_4	80,920	12.8	0.12045	0.12302	117,770	118,420
T_1	80,050	14.0	0.13102	0.1269	119,100	118,100
T_2	72,470	16.6	0.15357	0.15060	112,670	112,040
V_1	73,330	17.6	0.16212	0.15464	115,830	114,240
V_2	77,420	14.0	0.13102	0.13193	115,190	115,400
V_4	73,310	19.3	0.17645	0.1699	118,780	117,420

Table 10. Tensile Test Results Related to Necking:
Cold Work -Hot Work, Longitudinal Specimens

Code	Ultimate Tensile Strength, psi	ε_{UTS} Uniform Elongation, %	n Strain Hardening Exponent, UTS	n Strain Hardening Exponent, Graph	K Strength Coefficient, UTS psi	K Strength Coefficient, Graph psi
B_1	102,150	0.4	0.003992	--	104,840	--
B_2	102,490	0.45	0.004490	--	105,480	--
C_1	126,330	3.2	0.031499	0.04343	145,380	151,200
C_2	123,970	2.8	0.027615	0.03820	140,720	145,910
D_1	106,540	5.4	0.052592	0.05181	131,100	130,800
D_2	107,150	5.5	0.05354	0.06684	132,220	137,270
E_1	92,540	8.1	0.077886	0.09459	122,040	127,140
E_2	92,090	7.6	0.07325	0.08321	120,000	123,080
F_1	74,220	11.3	0.10706	0.10479	104,920	104,400
F_2	74,270	11.7	0.11064	0.11327	105,840	106,450
G_1	84,020	13.7	0.12839	0.1333	124,340	125,590
G_2	82,090	15.0	0.13976	0.14066	124,280	124,510
H_1	76,440	18.4	0.16890	0.17366	122,210	123,250
H_2	76,800	18.2	0.16721	0.16517	122,420	121,970
I_1	77,740	12.8	0.12045	0.11904	113,150	112,820
I_2	84,100	11.3	0.10706	0.1074	118,910	119,000
I_4	72,390	18.2	0.16721	0.15513	115,390	112,920
J_1	85,090	11.8	0.11154	0.11570	121,490	122,600
J_2	75,210	17.1	0.15786	0.14640	117,870	115,320
K_1	75,500	15.1	0.14063	0.13353	114,510	112,900
K_2	81,590	11.0	0.10436	0.10554	114,660	114,920
K_4	74,890	15.2	0.14150	0.14644	113,770	114,860

Table 11. Tensile Test Results Related to Necking:
Isothermal, Transverse Specimens

Code	Ultimate Tensile Strength, psi	ε_{UTS} Uniform Elongation, %	n Strain Hardening Exponent, UTS	n Strain Hardening Exponent, Graph	K Strength Coefficient, UTS psi	K Strength Coefficient, Graph psi
A_3	73,680	18.1	0.16636	0.17416	117,260	118,900
L_3	126,030	3.0	0.029559	0.050	144,050	153,900
M_3	114,250	4.7	0.045929	0.08287	137,800	152,570
N_3	97,990	6.0	0.058269	0.061069	122,580	123,550
O_3	84,990	7.7	0.074179	0.070866	111,010	110,050
P_3	78,760	15.9	0.14756	0.1555	121,070	122,890
R_3	86,000	12.0	0.11333	0.10619	123,280	121,350
S_3	79,650	14.7	0.13715	0.13598	119,970	119,690
T_3	72,990	17.4	0.16042	0.16509	114,930	115,910
V_3	72,870	18.0	0.16551	0.15909	115,810	114,460

Table 12. Tensile Test Results Related to Necking:
Cold Work - Hot Work, Transverse Specimens

Code	Ultimate Tensile Strength, psi	ε_{UTS} Uniform Elongation, %	n Strain Hardening Exponent, UTS	n Strain Hardening Exponent, Graph	K Strength Coefficient, UTS psi	K Strength Coefficient, Graph psi
B_3	101,620	2.1	0.020783	0.02788	112,420	115,460
B_5	101,620	2.2	0.021761	0.021521	112,880	112,770
C_3	127,050	3.3	0.032467	0.056625	146,650	158,200
D_3	109,380	5.2	0.050693	0.058215	133,850	136,820
E_3	90,780	6.8	0.065788	0.07278	115,970	118,140
F_3	74,780	11.8	0.11154	0.10309	106,780	104,780
G_3	86,130	14.3	0.13366	0.13139	128.840	128,240
H_3	74,890	16.8	0.15529	0.15581	116,810	116,930
I_3	75,280	14.7	0.13715	0.13333	113,390	112,530
I_5	72,590	18.7	0.17143	0.16627	116,590	115,510
J_3	82,080	9.8	0.09349	0.11080	112,470	117,000
K_3	75,610	15.7	0.14583	0.13100	115,840	112,480
K_5	76,800	13.5	0.12663	0.11983	113,240	111,640

Table 13. Tensile Test Results Related to Fracture:
Isothermal, Longitudinal Specimens

Code	Finishing Temperature °F	Engineering Fracture Stress psi	True Fracture Stress psi	Reduction of Area %	Elongation %
A_1	Mill	50,525	172,750	70.8	32.8
A_2	Mill	50,568	165,120	69.4	30.6
L_1	800	85,790	175,570	51.1	10.4
L_2	800	87,030	183,500	52.6	10.2
M_1	950	87,100	182,250	52.2	12.5
M_2	950	75,210	173,510	56.7	12.2
M_4	950	81,820	174,870	53.2	12.2
N_1	1100	68,740	166,410	58.7	16.7
N_2	1100	68,110	168,960	59.7	16.2
O_1	1250	59,210	166,480	64.4	20.6
O_2	1250	58,830	164,310	64.2	19.4
P_1	1400	53,510	166,580	67.9	28.0
P_2	1400	54,670	176,720	69.1	26.6
R_1	1550	52,210	187,880	72.2	28.0
R_2	1550	50,810	166,670	69.5	27.4
R_4	1550	52,340	181,240	71.1	26.2
S_1	1700	54,530	171,060	68.1	26.1
S_2	1700	50,100	154,220	67.5	29.6
S_4	1700	52,540	180,300	70.9	24.8
T_1	1850	50,570	167,110	69.7	29.2
T_2	1850	49,660	161,500	69.3	29.3
V_1	2000	50,530	170,070	70.3	30.2
V_2	2000	48,150	170,630	71.8	26.6
V_4	2000	49,550	163,780	69.7	36.3

Table 14. Tensile Test Results Related to Fracture:
Cold Work -Hot Work, Longitudinal Specimens

Code	Finishing Temperature °F	Engineering Fracture Stress psi	True Fracture Stress psi	Reduction of Area %	Elongation %
B_1	Cold Rolled	66,520	175,210	62.0	10.7
B_2	Cold Rolled	67,460	167,020	59.6	10.4
C_1	800	91,400	184,510	50.5	10.1
C_2	800	89,950	177,370	49.3	9.9
D_1	950	76,750	172,510	55.5	13.7
D_2	950	78,060	174,280	55.2	13.7
E_1	1100	63,590	172,670	63.2	18.6
E_2	1100	63,560	159,970	60.3	17.9
F_1	1250	48,240	168,510	71.4	24.0
F_2	1250	49,900	174,250	71.4	24.7
G_1	1400	56,370	194,810	71.1	25.6
G_2	1400	55,010	184,630	70.2	27.3
H_1	1550	52,120	173,430	69.9	32.1
H_2	1550	52,690	179,030	70.6	32.2
I_1	1700	51,100	172,940	70.4	25.1
I_2	1700	52,420	175,250	70.1	24.1
I_4	1700	50,190	161,780	69.0	31.0
J_1	1850	52,780	173,280	69.5	24.3
J_2	1850	51,100	163,310	68.7	29.8
K_1	2000	51,290	162,340	68.4	27.4
K_2	2000	50,090	183,280	72.7	25.4
K_4	2000	51,800	142,970	63.8	27.6

Table 15. Tensile Test Results Related to Fracture:
Isothermal, Transverse Specimens

Code	Finishing Temperature °F	Engineering Fracture Stress psi	True Fracture Stress psi	Reduction of Area %	Elongation %
A_3	Mill	58,660	154,950	62.1	28.3
L_3	800	104,210	158,170	34.1	6.8
M_3	950	93,370	153,140	39.0	9.8
N_3	1100	79,310	138,810	42.9	12.8
O_3	1250	67,280	139,460	51.8	16.3
P_3	1400	65,860	159,030	58.6	25.6
R_3	1550	67,450	151,390	55.4	21.8
S_3	1700	63,610	167,420	62.0	24.9
T_3	1850	50,570	116,050	56.4	31.0
V_3	2000	49,250	115,230	57.3	31.3

Table 16. Tensile Test Results Related to Fracture:
Cold Work -Hot Work, Transverse Specimens

Code	Finishing Temperature °F	Engineering Fracture Stress psi	True Fracture Stress psi	Reduction of Area %	Elongation %
B_3	Cold Rolled	74,530	141,480	47.3	9.4
B_5	Cold Rolled	77,570	141,850	45.3	9.2
C_3	800	102,960	160,190	35.7	7.5
D_3	950	90,170	147,900	39.0	10.2
E_3	1100	70,120	147,390	52.4	14.8
F_3	1250	48,180	139,930	65.6	25.1
G_3	1400	68,210	186,690	63.5	24.0
H_3	1550	59,430	150,550	60.5	27.2
I_3	1700	60,340	149,740	59.7	25.0
I_5	1700	50,030	163,830	69.7	32.7
J_3	1850	64,350	168,290	61.8	19.4
K_3	2000	51,080	165,960	69.2	27.8
K_5	2000	57,600	150,350	61.7	24.6

Table 17. Charpy Test Results: Isothermal Specimens

Code	Temperature, °F	Energy, ft. lb.	Code	Temperature, °F	Energy, ft. lb.
A_1	-125	2	L_6	-105	1.5
A_6	-105	17	L_7	3	2
A_{11}	-100	10	L_3	32	7
A_2	-88	5	L_8	55	5.5
A_{10}	-75	12	L_4	75	10
A_9	-50	19	L_1	81	8
A_8	-25	26	L_{11}	87	18
A_7	3	36	L_9	100	16
A_3	32	46	L_2	112	19
A_4	75	46	L_{10}	125	18
A_5	212	47	L_5	212	17
M_6	-105	2	N_6	-105	1.5
M_{10}	-75	1	N_{10}	-75	1.0
M_9	-50	1.5	N_9	-50	2.0
M_8	-25	7.5	N_1	-37	1.0
M_{11}	-12	2	N_8	-25	13
M_7	3	20	N_{11}	-12	14
M_1	17	19	N_7	3	7.5
M_3	32	17	N_2	16	23
M_2	55	21	N_3	32	19
M_4	75	21	N_4	75	23
M_5	212	21	N_5	212	24

(Continued)

Table 17. Charpy Test Results: Isothermal Specimens
(Continued)

Code	Temperature, °F	Energy, ft. lb.	Code	Temperature, °F	Energy, ft. lb.
O_6	-105	1.0	P_6	-105	15
O_{10}	-75	1.0	P_{11}	-100	1.0
O_9	-50	2.0	P_2	-88	2.5
O_2	-37	2.5	P_{10}	-75	4.0
O_8	-25	15	P_1	-62	10
O_1	-19	20	P_9	-50	20
O_{11}	-12	7	P_8	-25	21
O_7	3	19	P_7	3	41
O_3	32	26	P_3	32	36
O_4	75	31	P_4	75	36
O_5	212	25	P_5	212	36
R_{11}	-150	2	S_{11}	-150	1
R_1	-125	1	S_1	-125	4
R_6	-105	16	S_6	-105	22
R_2	-88	20	S_2	-88	19
R_{10}	-75	20	S_{10}	-75	22
R_9	-50	29	S_9	-50	27
R_8	-25	43	S_8	-25	52
R_7	3	40	S_7	3	38
R_3	32	45	S_3	32	46
R_4	75	46	S_4	75	42
R_5	212	44	S_5	212	47

(Continued)

Table 17. Charpy Test Results: Isothermal Specimens
(Continued)

Code	Temperature, °F	Energy ft. lb.	Code	Temperature, °F	Energy, ft. lb.
T_1	-125	1	V_6	-105	4
T_6	-105	20	V_2	-88	2
T_{11}	-100	1	V_{10}	-75	4
T_2	-88	28	V_{11}	-62	29
T_{10}	-75	23	V_9	-50	22
T_9	-50	25.5	V_8	-25	30
T_8	-25	36	V_1	-12	35
T_7	3	50	V_7	3	53
T_3	33	47	V_3	32	54
T_4	75	48	V_4	75	53
T_5	212	58	V_5	212	56

Table 18. Charpy Test Results:
Cold Work - Hot Work Specimens

Code	Temperature, °F	Energy ft. lb.	Code	Temperature, °F	Energy, ft. lb.
B_6	-105	1.5	C_6	-105	1
B_{10}	-75	2.5	C_7	3	3
B_9	-50	4.5	C_3	32	2.5
B_2	-37	2.5	C_8	55	5
B_8	-25	13	C_4	75	11
B_1	-19	11	C_1	87	20
B_{11}	-12	2	C_9	100	4
B_7	3	21	C_{11}	100	11
B_3	32	19	C_2	112	12
B_4	75	21	C_{10}	125	17
B_5	212	27	C_5	212	17

(Continued)

Table 18. Charpy Test Results: Cold Work –Hot Work Specimens
(Continued)

Code	Temperature, °F	Energy, ft. lb.	Code	Temperature, °F	Energy, ft. lb.
D_6	-105	2	E_6	-105	1.5
D_{10}	-75	1	E_{10}	-75	1.0
D_9	-50	2	E_9	-50	2.0
D_8	-25	4	E_2	-32	1.5
D_{11}	-12	2	E_8	-25	3
D_1	-6	10	E_1	-12	6
D_7	3	16	E_{11}	-12	15
D_2	17	16	E_7	3	23
D_3	32	17	E_3	32	28
D_4	75	19	E_4	75	27
D_5	212	20	E_5	212	30
F_6	-105	1	G_6	-105	1
F_{10}	-75	1	G_1	-88	2
F_9	-50	2	G_{10}	-75	19
F_8	-25	8	G_{11}	-62	14
F_2	-19	3	G_9	-50	20
F_{11}	-12	7	G_8	-25	22
F_1	-6	7	G_7	3	27
F_7	3	27	G_3	32	41
F_3	32	38	G_2	55	41.5
F_4	75	42	G_4	75	43
F_5	212	43	G_5	212	39

(Continued)

Table 18. Charpy Test Results: Cold Work –Hot Work Specimens
(Continued)

Code	Temperature, °F	Energy, ft. lb.	Code	Temperature, °F	Energy, ft. lb.
H_1	-125	2	I_1	-125	1
H_{11}	-150	2	I_6	-105	19
H_6	-105	19	I_{11}	-100	24
H_2	-88	22	I_2	-88	4.5
H_{10}	-75	22	I_{10}	-75	25
H_9	-50	24	I_9	-50	17
H_8	-25	47	I_8	-25	51
H_7	3	53	I_7	3	33
H_3	32	44	I_3	32	52
H_4	75	46	I_4	75	45
H_5	212	47	I_5	212	44
J_6	-105	24	K_6	-105	2.5
J_{11}	-100	1	K_{10}	-75	1.0
J_2	-88	2	K_2	-70	2.0
J_{10}	-75	3.5	K_1	-60	1.0
J_1	-62	16	K_9	-50	27
J_9	-50	23	K_{11}	-37	16
J_8	-25	25	K_8	-25	30
J_7	3	31	K_7	3	37
J_3	32	44	K_3	32	49
J_4	75	57	K_4	75	64
J_5	212	49	K_5	212	60

Table 19. V-Notch Charpy Transition Temperatures, °F:
Isothermal Specimens

Code	Finishing Temperature °F	15 ft. lb. Transition Temperature, °F
A	Mill	-57.5
L	800	108
M	950	6
N	1100	-11.5
O	1250	-11.5
P	1400	-51.5
R	1550	-107.5
S	1700	-96
T	1850	-70
V	2000	-57.5

Table 20. V-Notch Charpy Transition Temperatures, °F:
Cold Work - Hot Work Specimens

Code	Finishing Temperature °F	15 ft. lb. Transition Temperature, °F
B	Cold Rolled	-5
C	800	83
D	950	2.5
E	1100	-7
F	1250	-8
G	1400	-71
H	1550	-112
I	1700	-77.5
J	1850	-61
K	2000	-38

Table 21. Optical Metallographic Observations
and Results: Isothermal Specimens

Code	Magnification Factor	d ferrite in $\times 10^4$	$d^{-1/2}$ ferrite $(in)^{-1/2}$	Percent Pearlite	Ω ferrite Degree of Orientation $\times 10$
$A(E_2)$	200X	7.05	37.66	29.5	0.93
$A(E_3)$	200X	7.19	37.28	29.1	1.45
$L(E_{22})$	200X	7.52	36.47	25.6	3.88
$L(E_{23})$	200X	7.38	36.82	24.8	3.70
$M(E_{62})$	200X	8.16	35.01	23.1	3.48
$M(E_{63})$	200X	8.43	34.43	21.8	4.12
$N(E_{26})$	200X	7.55	36.40	22.2	4.15
$N(E_{27})$	200X	7.55	36.40	21.4	4.41
$O(E_{65})$	200X	7.18	37.31	17.1	3.78
$O(E_{67})$	200X	7.10	37.54	20.5	4.11
$P(E_{72})$	400X	3.29	55.16	31.6	3.72
$R(E_{30})$	200X	6.55	39.09	29.9	1.99
$R(E_{31})$	200X	6.69	38.67	35.0	2.20
$S(E_{34})$	200X	8.14	35.05	25.2	1.42
$S(E_{35})$	200X	8.25	34.80	23.5	1.35
$T(E_{74})$	200X	7.82	35.81	37.6	1.73
$T(E_{75})$	200X	7.68	36.09	38.9	1.68
$V(E_{78})$	200X	10.68	30.69	41.9	0.92
$V(E_{79})$	200X	10.24	31.25	40.2	1.41

Table 22. Optical Metallographic Observations and Results: Cold Work-Hot Work Specimens

Code	Magnification Factor	d ferrite in x 10^4	$d^{-1/2}$ ferrite (in)$^{-1/2}$	Percent Pearlite	α ferrite Degree of Orientation x 10
B(E$_6$)	200X	8.80	33.71	27.8	2.73
B(E$_7$)	200X	8.58	34.14	29.9	2.82
C(E$_{38}$)	200X	11.93	28.96	23.5	3.64
C(E$_{39}$)	200X	11.88	29.02	23.9	3.58
D(E$_{14}$)	200X	10.15	31.39	21.4	5.02
D(E$_{15}$)	200X	9.8	31.94	22.6	4.64
E(E$_{10}$)	200X	9.65	32.19	31.6	4.73
E(E$_{11}$)	200X	10.10	31.47	29.9	5.22
F(E$_{41}$)	200X	11.71	29.23	23.5	4.19
F(E$_{42}$)	400X	8.25	34.82	34.6	4.77
G(E$_{48}$)	400X	4.93	45.03	30.3	3.92
G(E$_{47}$)	400X	4.90	45.20	29.9	3.83
H(E$_{54}$)	200X	8.63	34.03	25.6	3.12
H(E$_{55}$)	200X	8.62	34.05	26.1	2.52
I(E$_{18}$)	200X	10.60	30.71	29.9	0.87
I(E$_{19}$)	200X	10.34	31.09	30.3	1.12
J(E$_{50}$)	200X	12.36	28.45	25.2	0.28
J(E$_{52}$)	200X	11.09	30.03	26.9	0.65
K(E$_{58}$)	200X	10.28	31.19	58.1	2.29
K(E$_{59}$)	200X	9.74	32.05	59.8	1.93

CHAPTER V

CONCLUSIONS AND DISCUSSION

Isothermal Code Designations

The primary conclusion which was made after a study of the
results of experimentation included in Tables 3 through 22 was that
there is a rather narrow temperature range in which isothermal fabri-
cation may be accomplished with the result that many of the charac-
teristics desired for X-52 steel for structural applications will be
attractive. In other words, fabrication in this temperature range
will result in an optimum combination of properties. The applicable
temperature range is one which extends over a narrow width including
1550°F. That properties are desirable as a result of 1550°F iso-
thermal rolling is demonstrated by the following considerations, which
also allow many other conclusions to be made:

    a. Figure 2 shows that for longitudinal specimens there are
strong increases of yield strength with decreasing fabri-
cation temperatures below 1550°F. Ultimate tensile strength
apparently begins to greatly increase when the isothermal
fabrication temperature is below 1400°F. Figure 3 shows
similar behavior for transverse specimens.

    b. Variations of yield strength values resulting from changes
of isothermal fabrication temperatures are relatively small,
as compared with the previous Case a, when fabrication

temperatures are at or above 1550°F, as shown by Figures 2 and 3. In fact, it appears that if there were more available data for fabrication temperatures at or above 1550°F, that the construction of a Hall-Petch relationship for this temperature range would be warranted. That this is the case is demonstrated by Figure 4.

c. Rapid decrease of values of the strain hardening exponent n occur as the temperature of fabrication is lowered below 1400°F (Figure 5).

d. Values of the strength coefficient K increase as the isothermal fabrication temperature is lowered below 1200°F, as indicated by Figures 6 and 7.

e. Percent elongation and percent reduction of area, both of which are measures of ductility, continuously decrease in value as the isothermal fabrication temperature is lowered below 1400°F, the behavior being shown by Figures 8 and 9.

f. Isothermal fabrication in the vicinity of 1550°F produces X-52 plate with unusually desirable low temperature fracture characteristics; the 15 foot pound Charpy V-notch transition temperature may be as low as 107.5°F, which it was for "R" specimens (Figure 10).

g. The degree of orientation of ferrite grains strongly increases as the isothermal fabrication temperature is lowered below 1550°F, the behavior being illustrated by Figure 11.

As compared with the mill finished product designated as "A," the "R" material isothermally fabricated at 1550°F was harder, had increased values of both upper and lower yield strengths, had increased ultimate tensile strength, and had rather equivalent ductility, but the 15 foot-pound Charpy V-notch transition temperature was lowered by 50°F. At 1550°F, X-52 is only slightly above the A_3 line of the iron-iron carbide metastable equilibrium phase diagram. Hence, it is concluded that fabrication at this temperature results in an unusually effective high temperature thermomechanical treatment (HTTMT).

When isothermal fabrication is accomplished at temperatures below about 1400°F the rapid deterioration of properties with decreasing fabrication temperatures can be traced to increases in value of the friction stress σ_i. That the friction stress term does so increase in value is shown by consideration of the Hall-Petch equation and Figure 4. Increased values of σ_i resulting from low isothermal fabrication temperatures is consistent with all behavior shown by Figures 2 through 11. The effect is no doubt a result of cold work, although it would also be logical to assume that aging plays a possibly important part.

Study of the photomicrographs included in Figure 12, for codes P, R, and S which were immediately adjacent to each other on the fabrication temperature scale, substantiates many of the conclusions and postulations made in this chapter. The microstructure associated with "R" material, fabricated at 1550°F, is very desirable.

Hot Worked - Cold Worked Code Designations

A comparison of the test results shown by samples coded C, D,
E, F, G, H, I, J, and K, shown by Figures 13 through 22, with the
previously discussed results obtained with samples L, M, N, O, P, R,
S, T and V, shown by Figures 2 through 12, results in the conclusion
that there are but minimal differences between equivalent figures involved
with identical elevated temperature fabrication. It must be concluded
that the preliminary thermomechanical treatment (PTMT) attempted here
is not effective. Thermal effects in the heating furnace and/or
subsequent warm-hot fabrication apparently removes all traces of
previous cold work, a most important conclusion in itself.

Incidentally, it was found that for all of the code designa-
tions considered in this thesis, there was a rather linear relation-
ship between ultimate tensile strength and Brinell Hardness number
(Figure 23). Relationships of this type are often found, for a given
steel, when cold work alone is responsible for hardening.
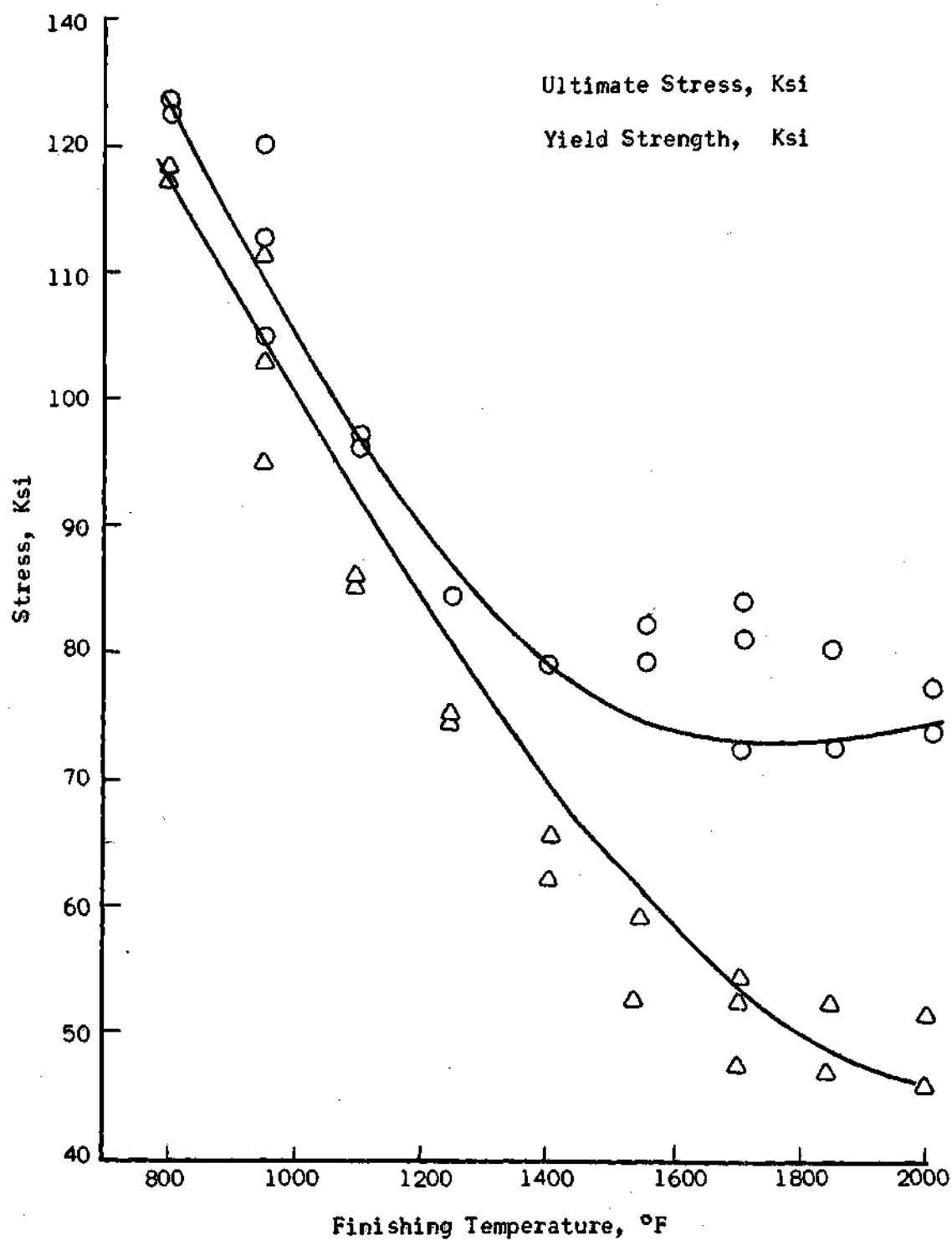
Figure 2. Ultimate Tensile Stress and Yield Strength as Functions of Finishing Temperature: Isothermal, Longitudinal Specimens.
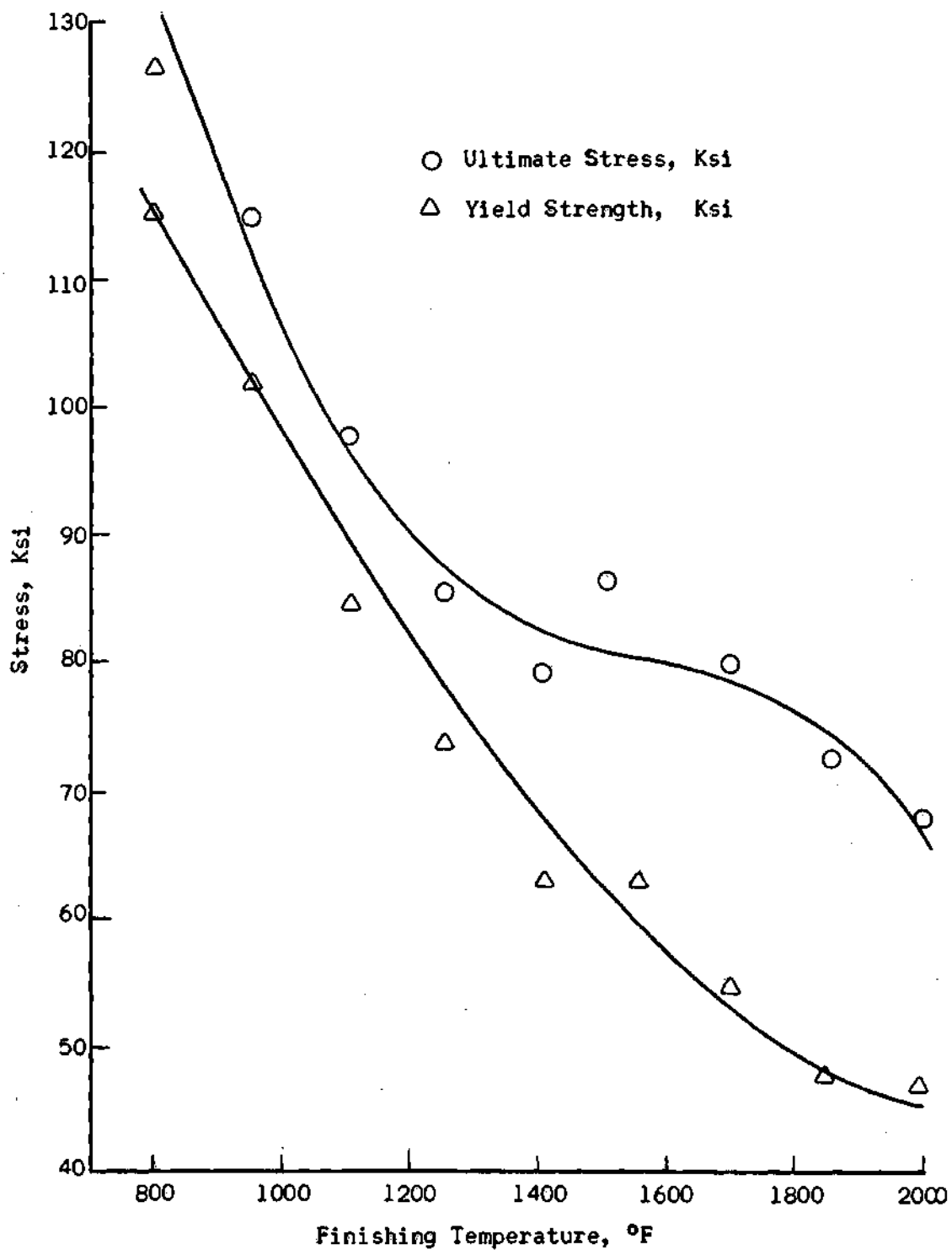
Figure 3. Ultimate Tensile Stress and Yield Strength as Functions
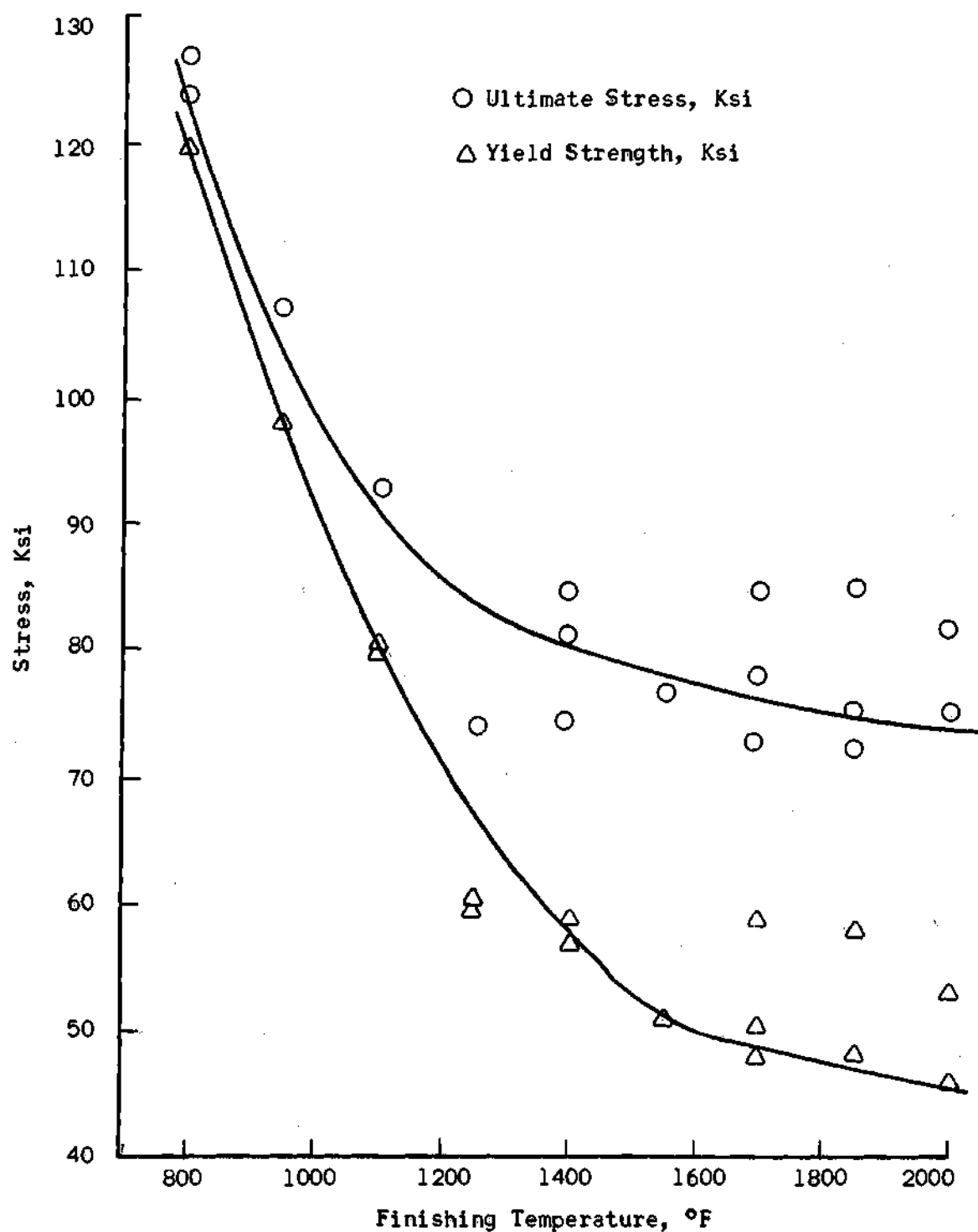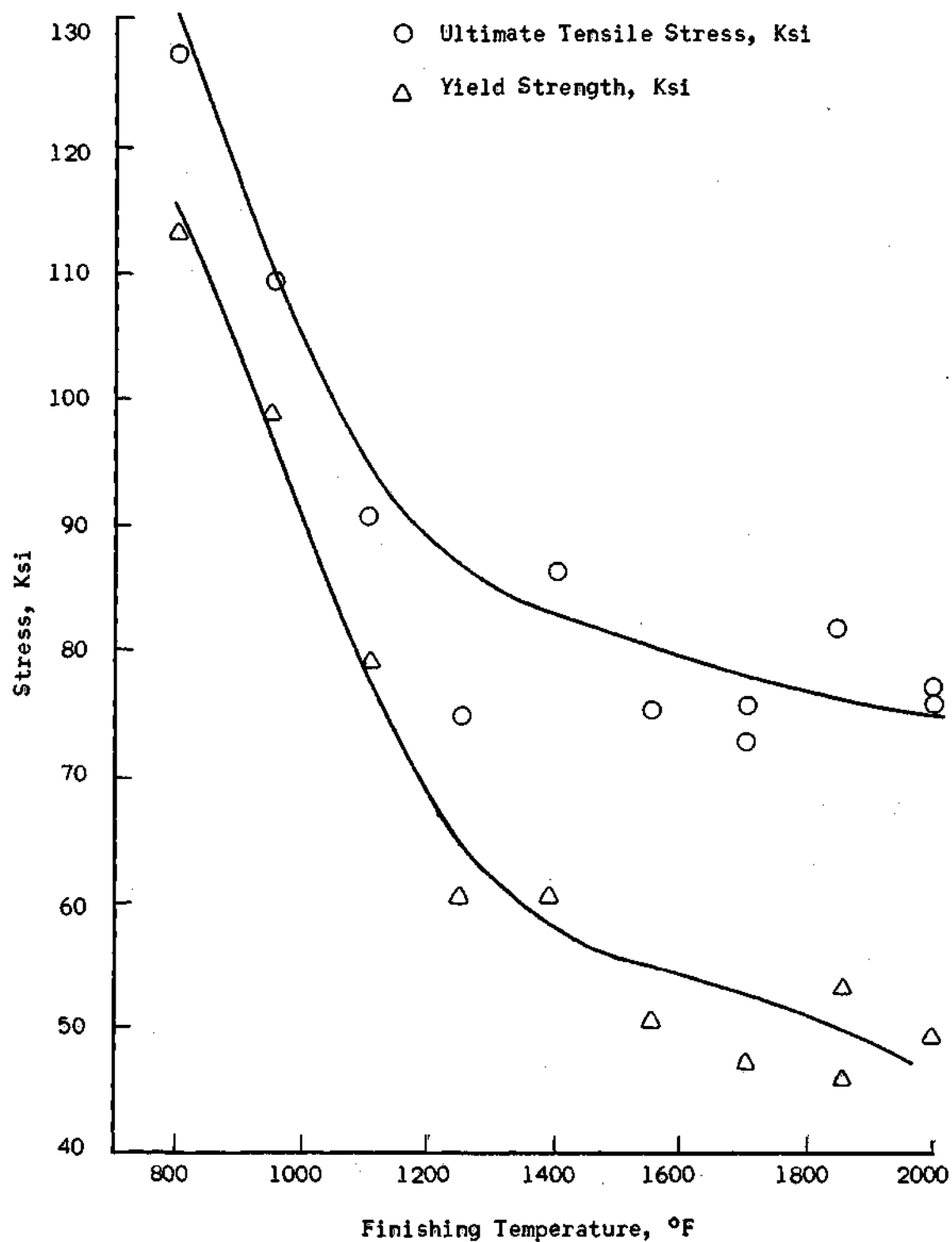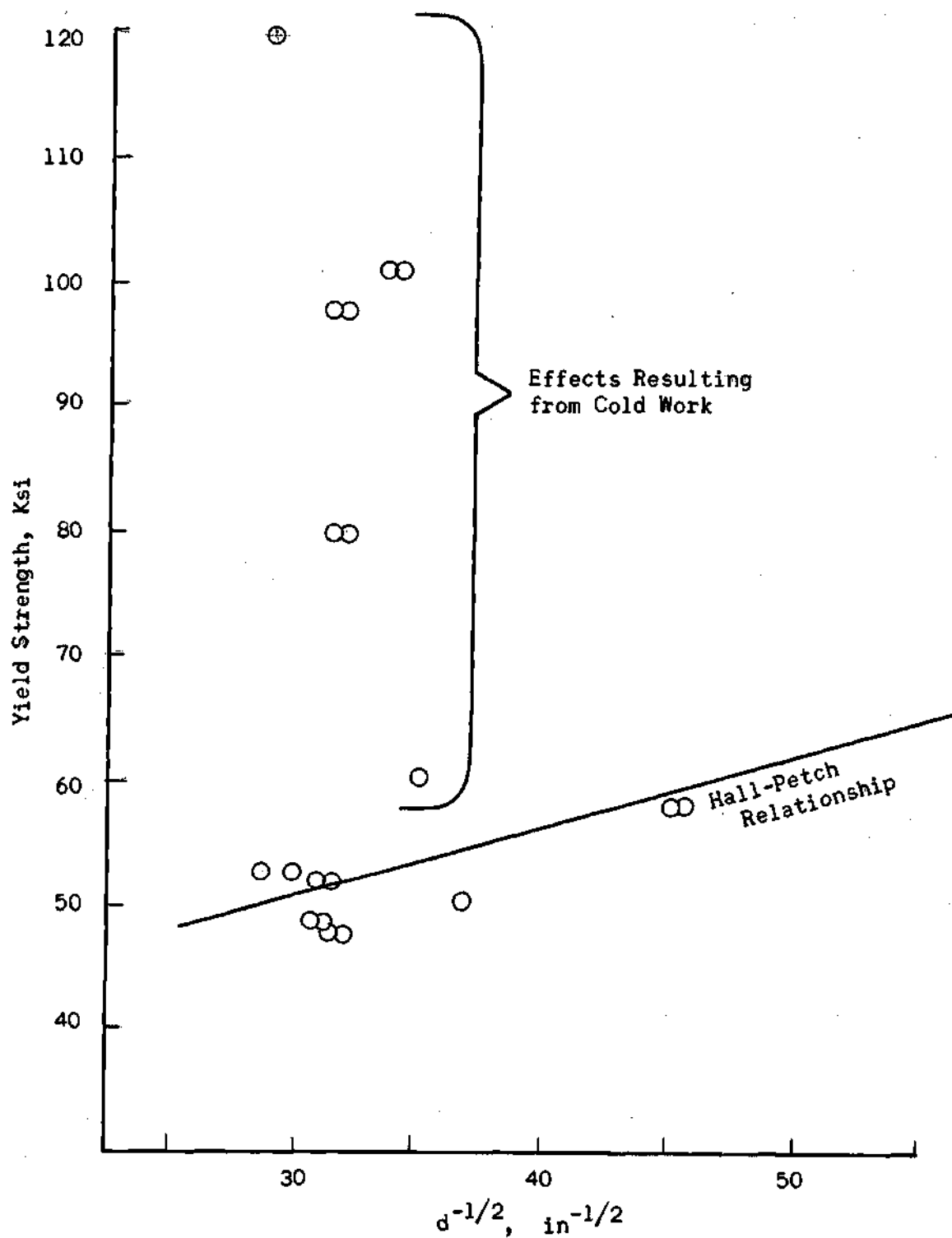of Finishing Temperature: Isothermal, Transverse
Specimens.
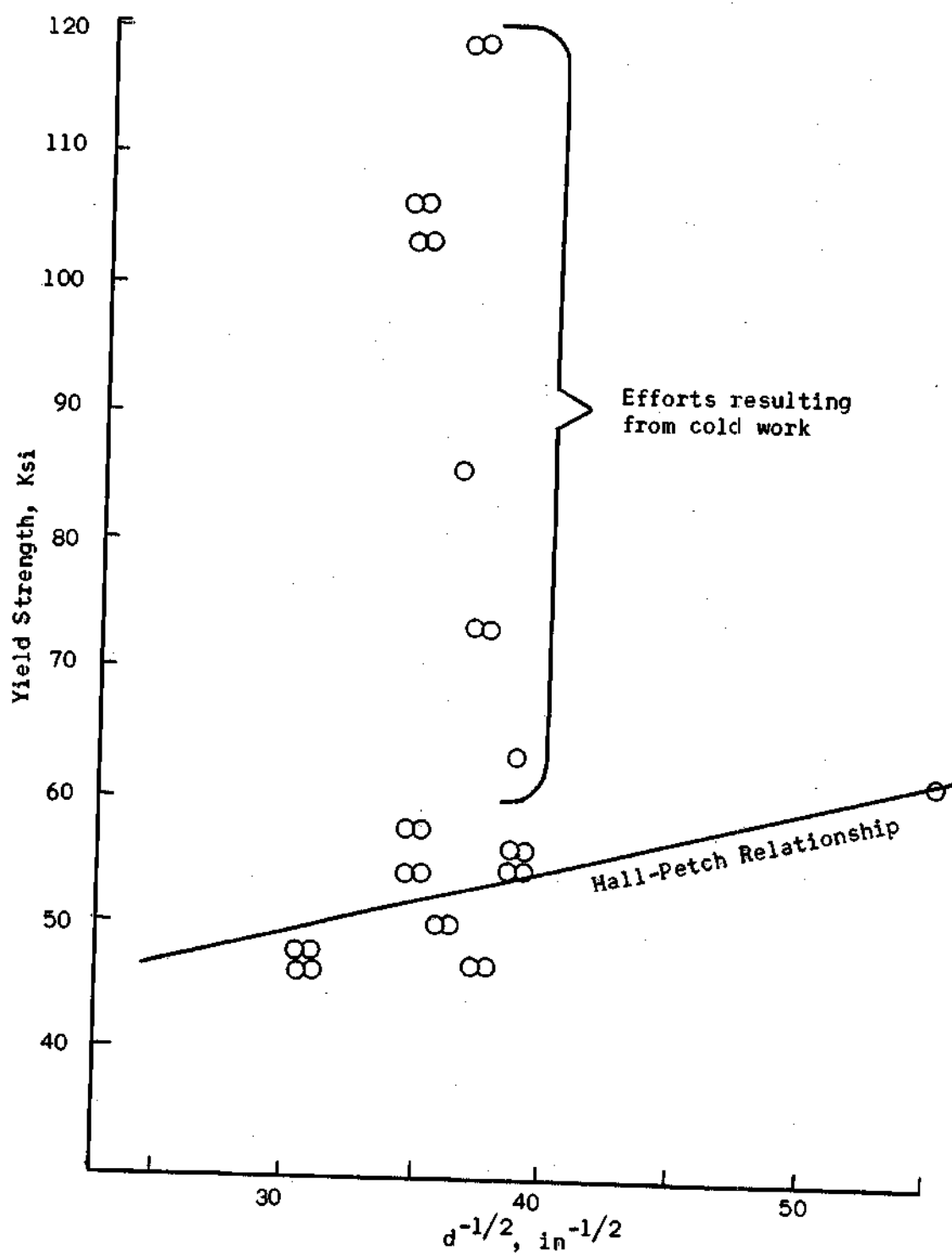
Figure 4.   Yield Strength as a Function of
$d^{-1/2}$ Isothermal Specimens.
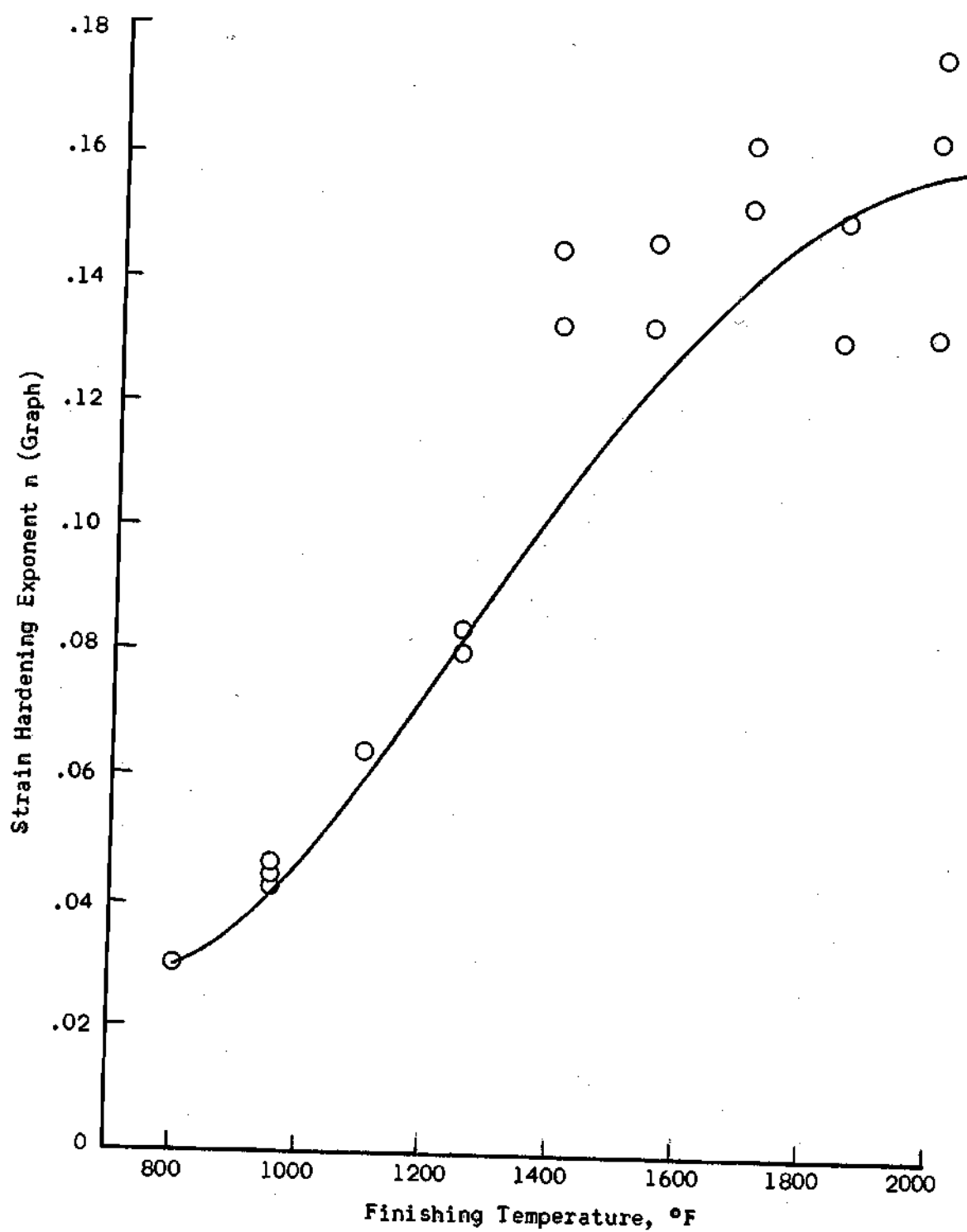
Figure 5. Strain Hardening Exponent n as a Function
of Finishing Temperature: Isothermal,
Longitudinal Specimens.
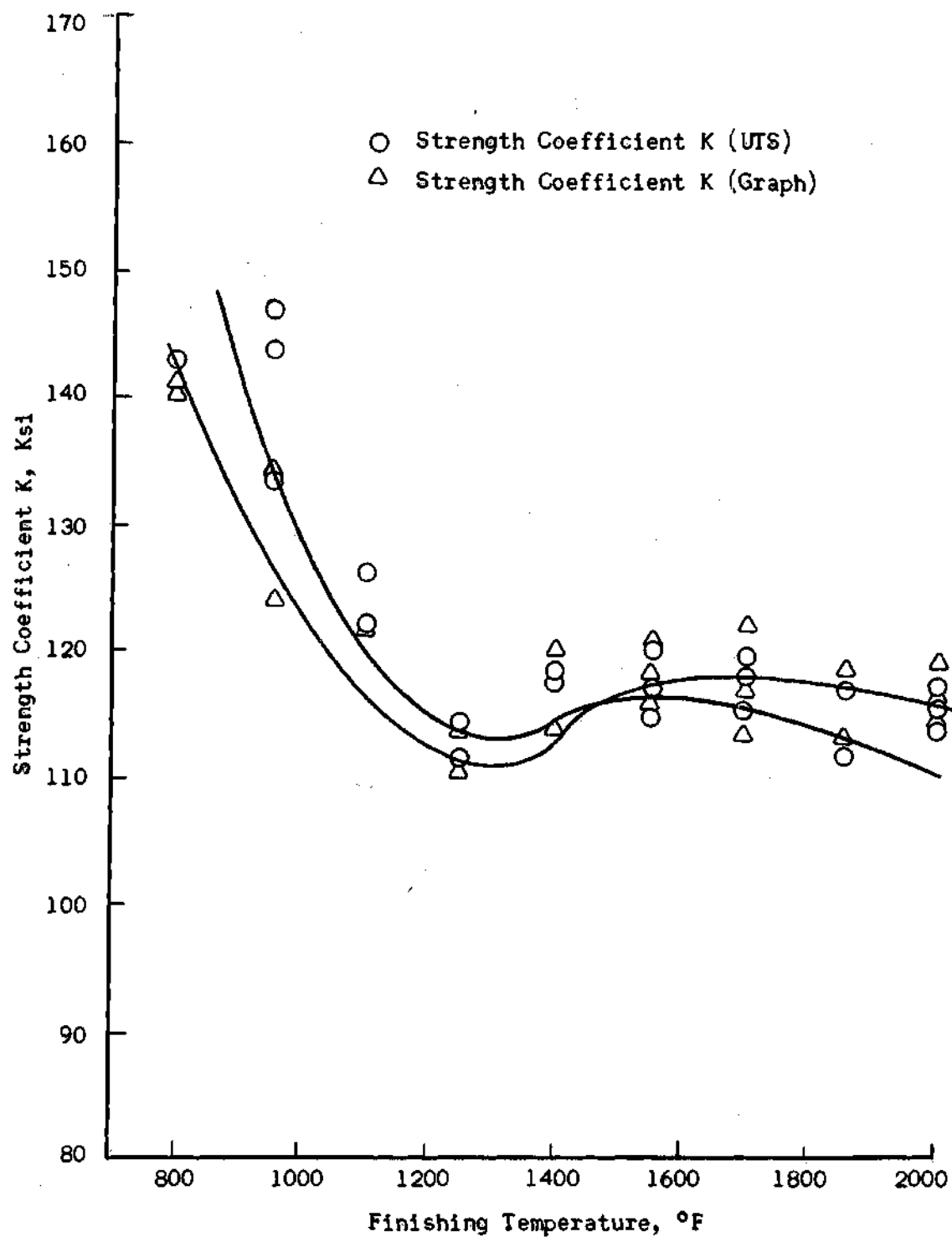
Figure 6. Strength Coefficient K as a Function of
Finishing Temperature: Isothermal,
Longitudinal Specimens.
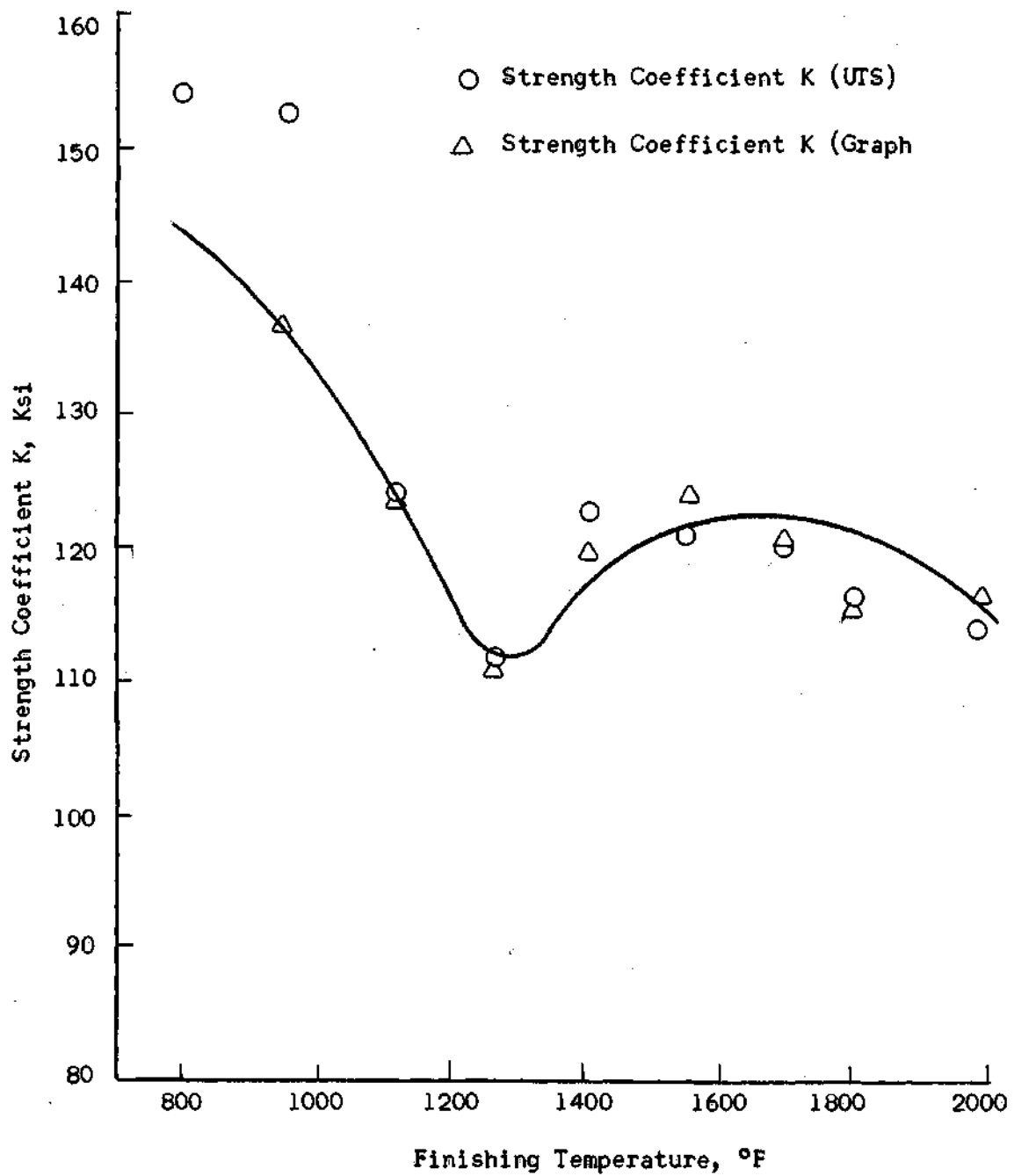
Figure 7. Strength Coefficient K as a Function of
Finishing Temperature: Isothermal,
Transverse Specimens
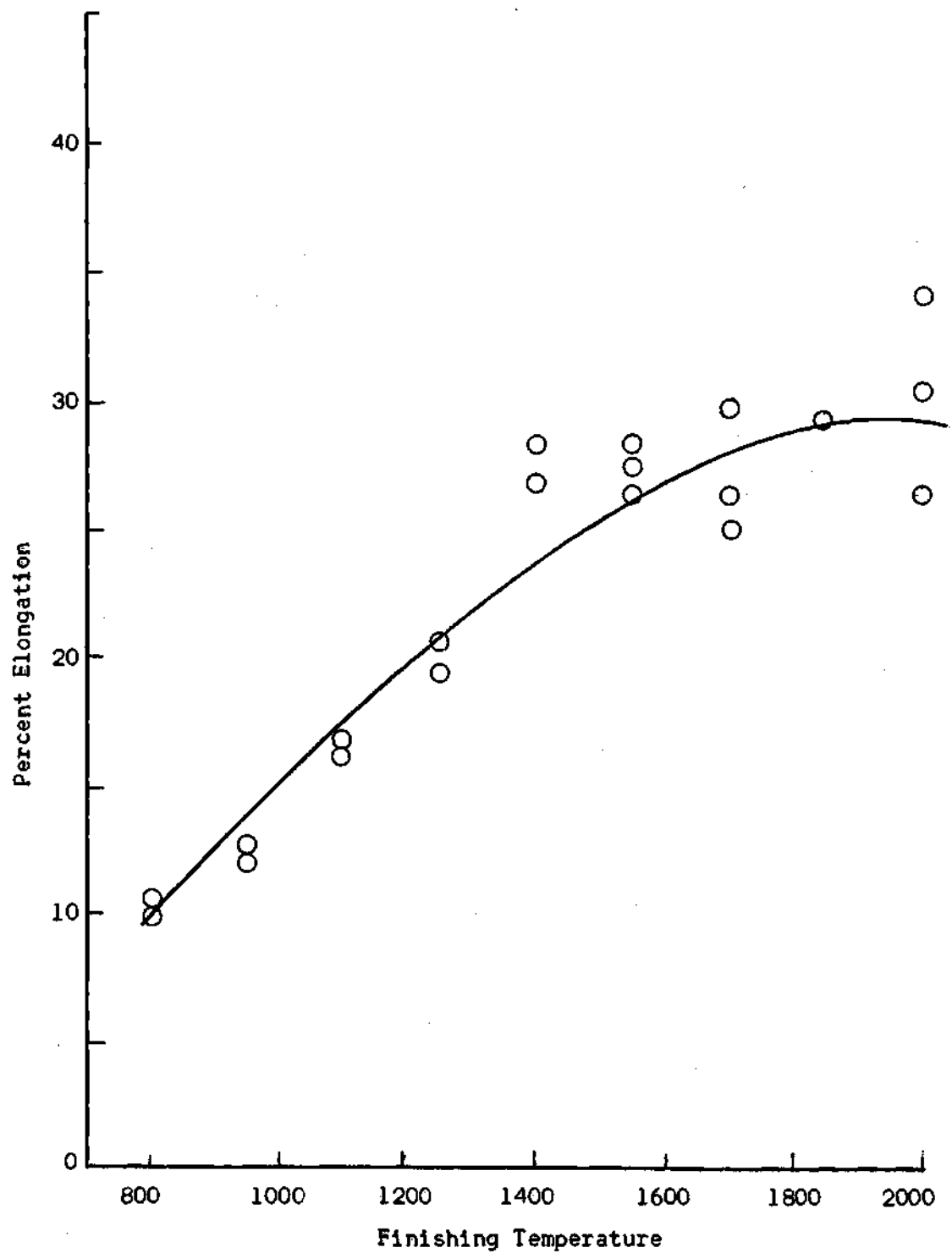
Figure 8. Percent Elongation as a Function of Finishing
Temperature: Isothermal, Longitudinal Specimens.
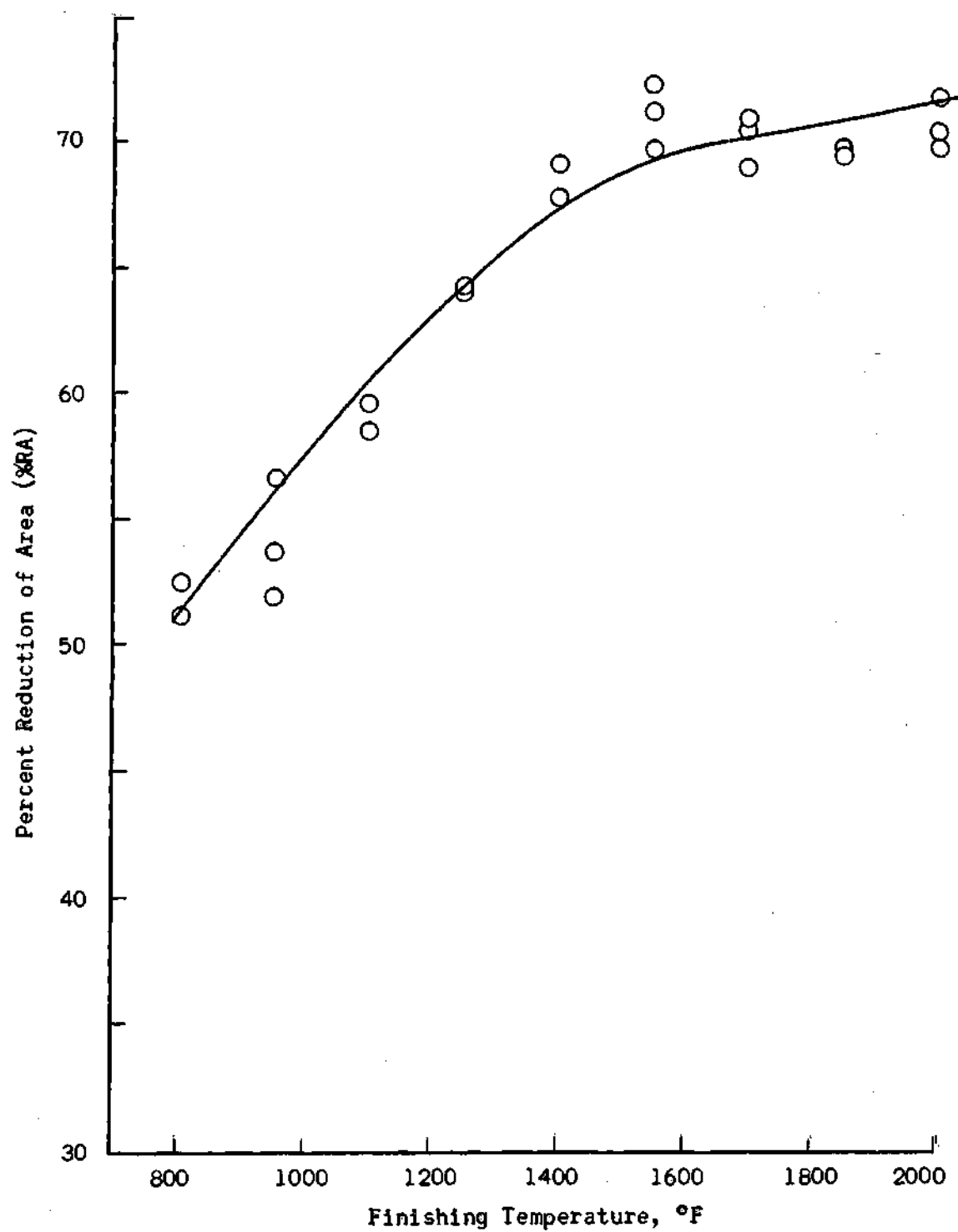
Figure 9.   Percent Reduction of Area as a Function
            of Finishing Temperature: Isothermal,
            Longitudinal Specimens.
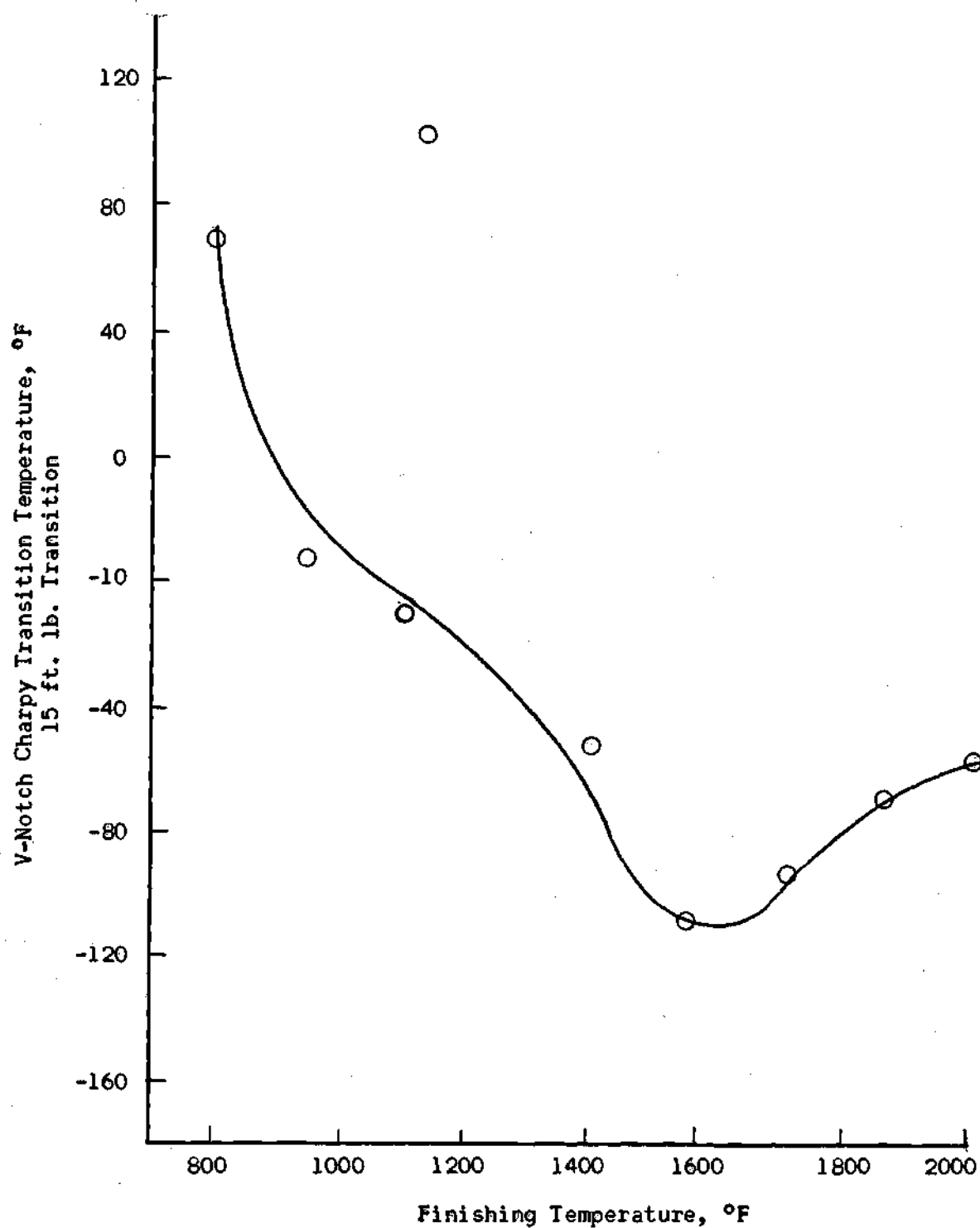
Figure 10. V-Notch Charpy Transition Temperature as a
Function of Finishing Temperature:
Isothermal Specimens.
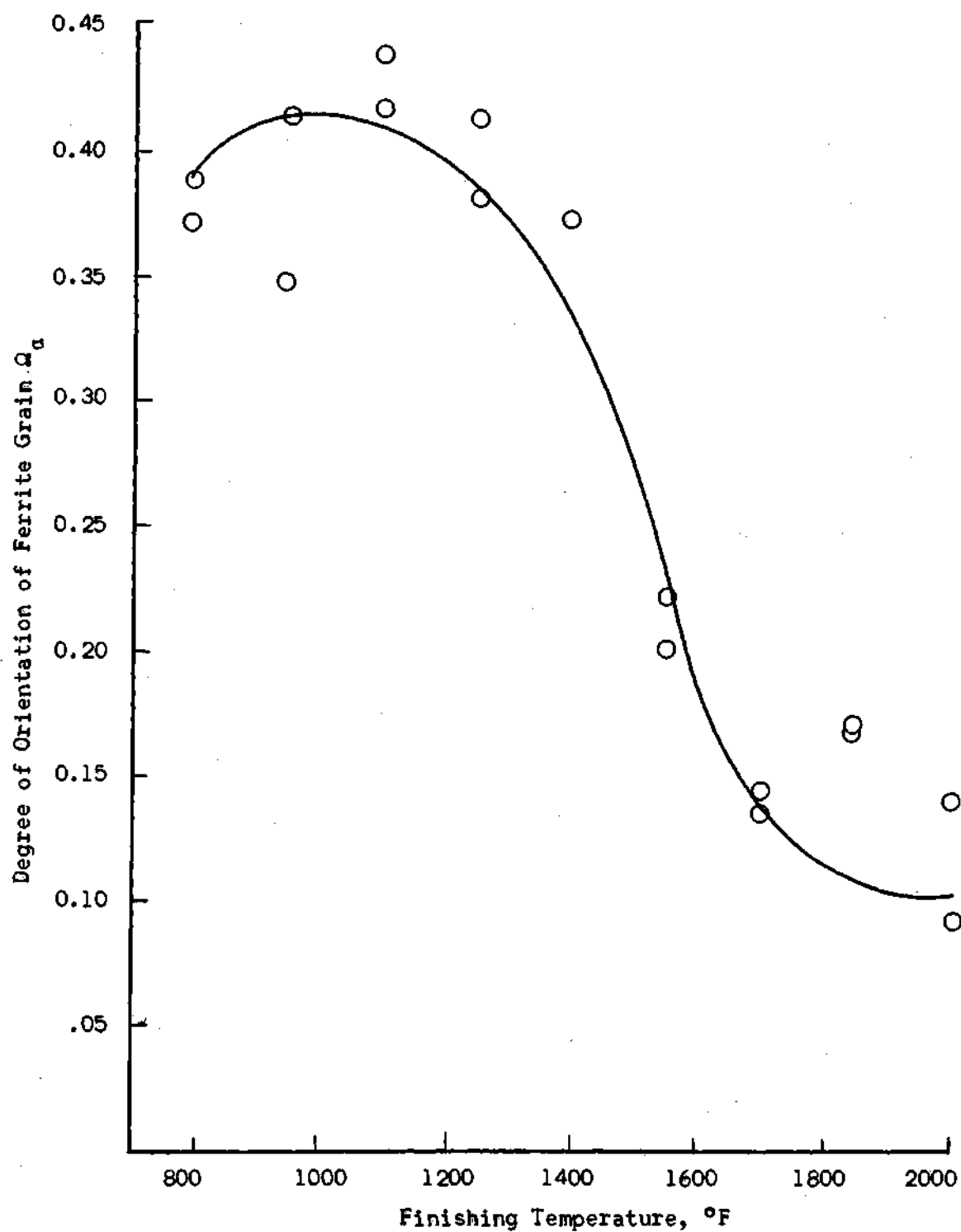
Figure 11. Degree of Orientation of Ferrite Grain as a
Function of Finishing Temperature:
Isothermal Specimens.
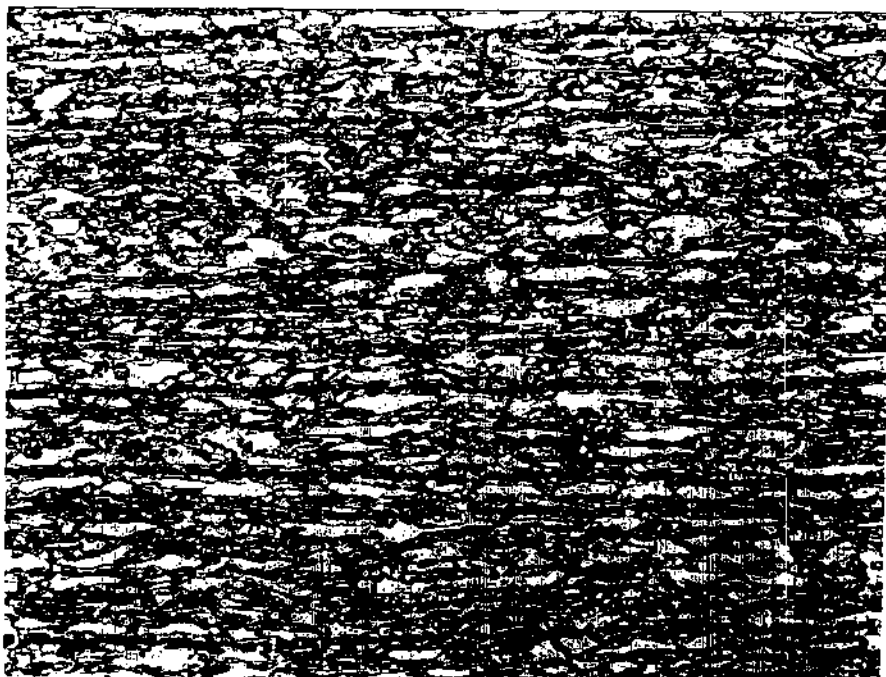
a. Photomicrograph of Specimen P, Fabricated
   at 1400°F, Magnification 200X

Figure 12. Optical Photomicrographs.
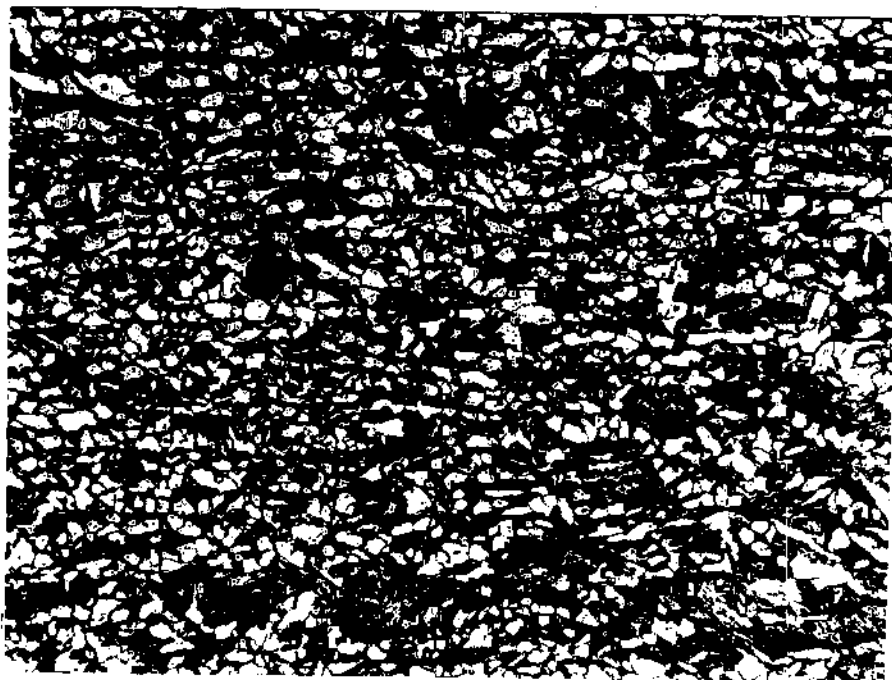
b. Photomicrograph of Specimen R, Fabricated
at 1550°F, Magnification 200X

Figure 12. Optical Photomicrographs.
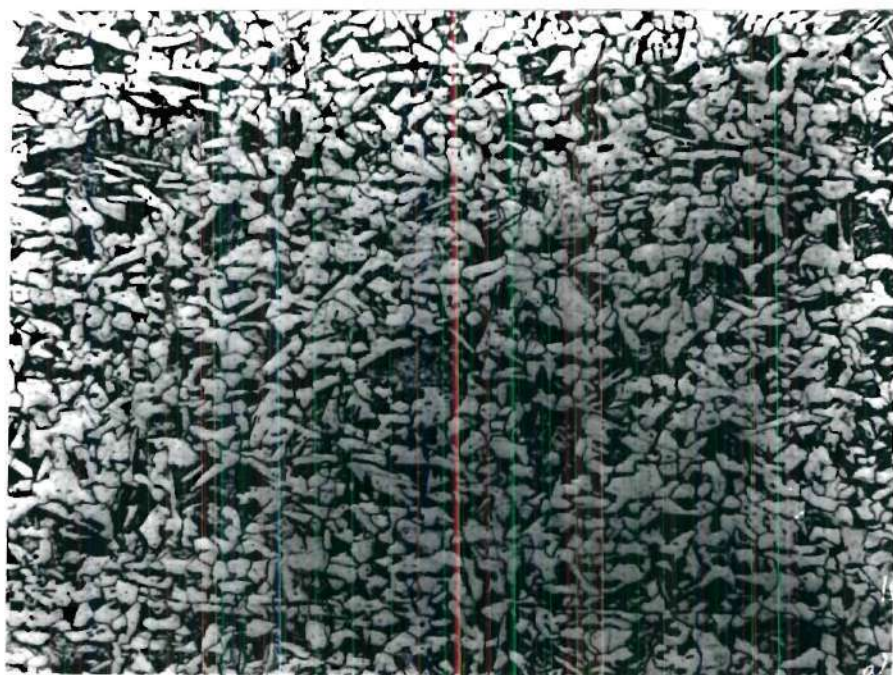
c. Photomicrograph of Specimen S, Fabricated
    at 1700°F, Magnification 200X.

Figure 12. Optical Photomicrographs.

Figure 13. Ultimate Tensile Stress and Yield Strength as
            Functions of Finishing Temperature: Cold Work -
            Hot Work, Longitudinal Specimens.

Figure 14. Ultimate Tensile Stress and Yield Strength as
Functions of Finishing Temperature: Cold
Work -Hot Work, Transverse Specimens.

Figure 15. Yield Strength as a Function of $d^{-1/2}$, Cold Work - Hot Work Specimens.
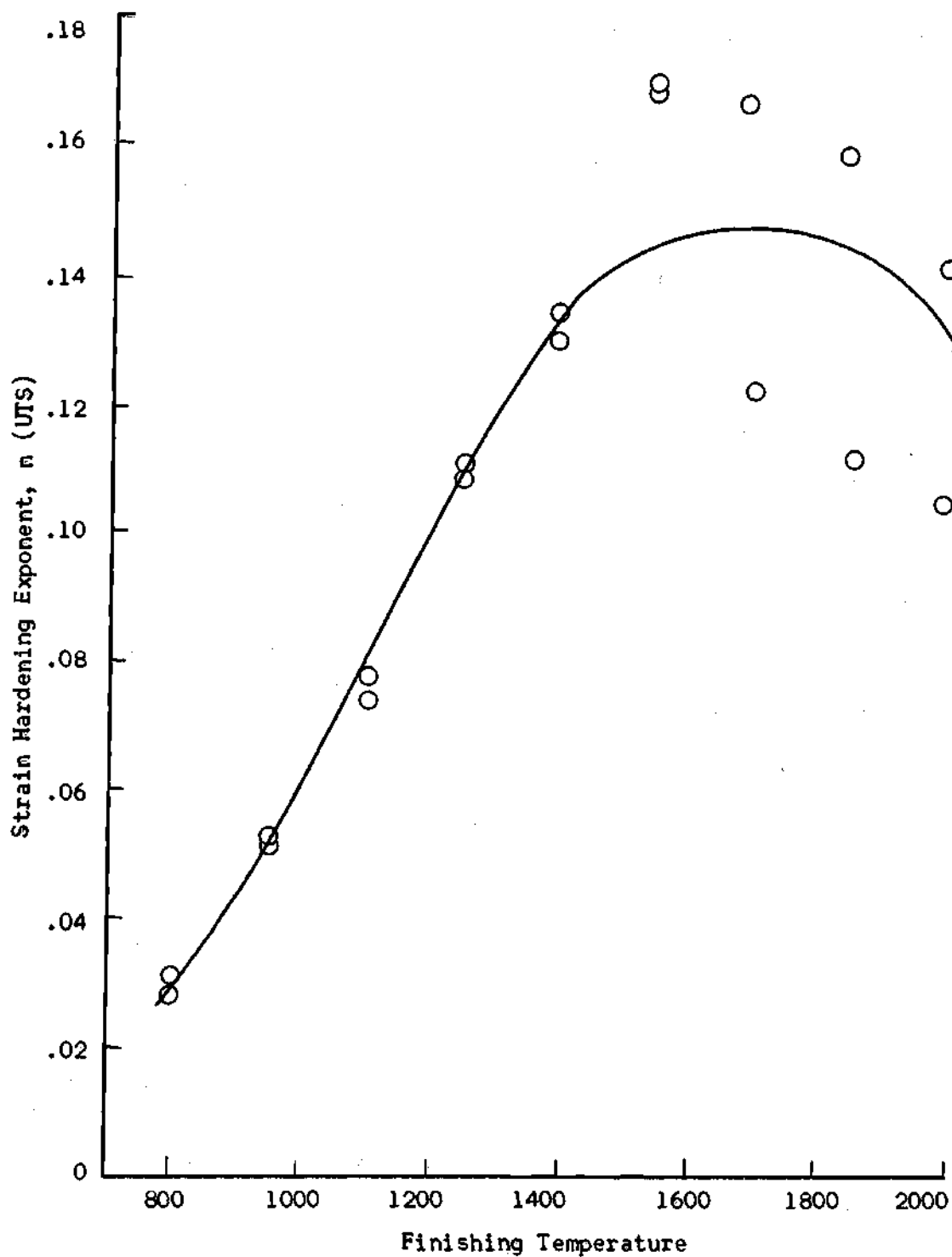
Figure 16. Strain Hardening Exponent n as a Function of
Finishing Temperature: Cold Work - Hot Work,
Longitudinal Specimens.
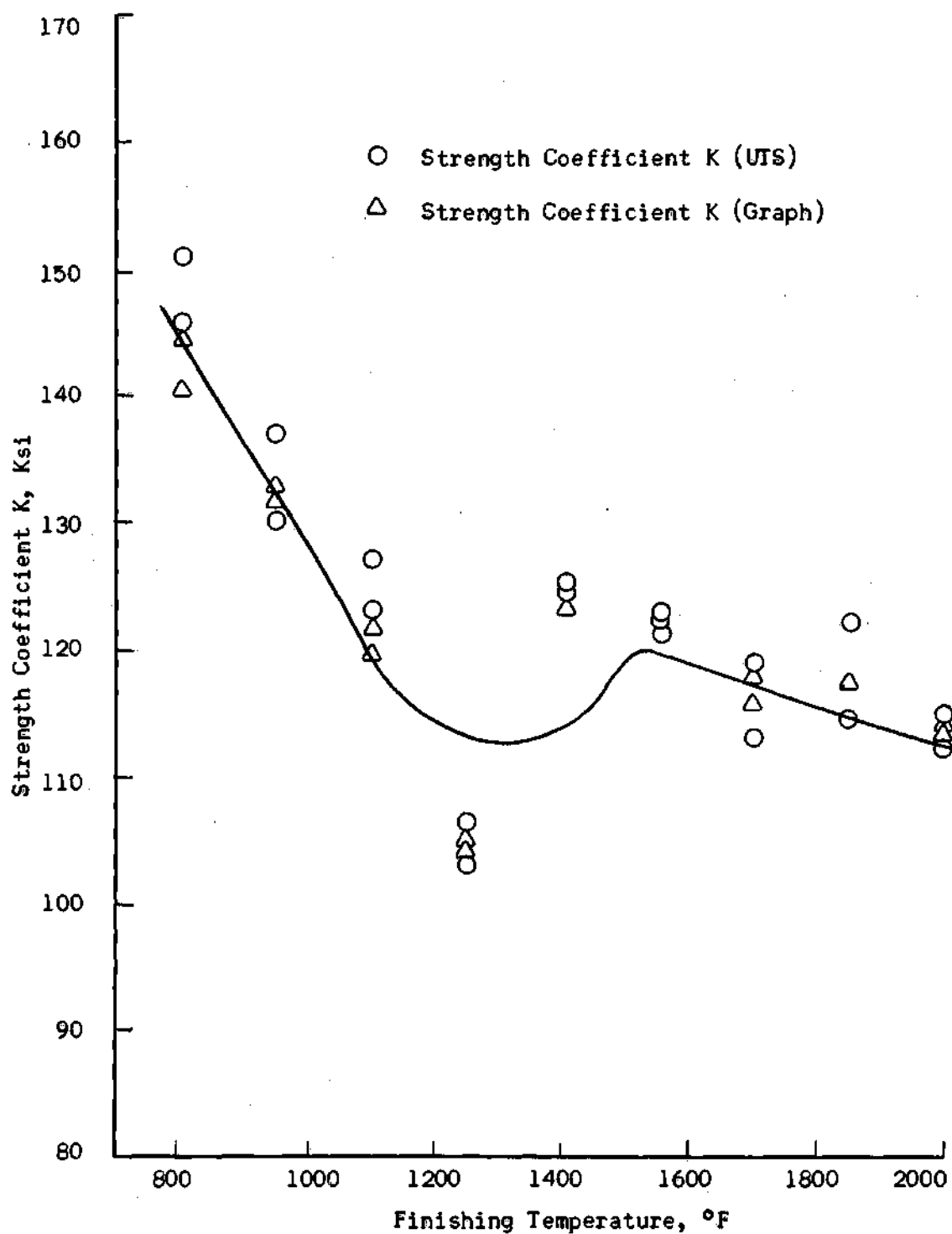
Figure 17. Strength Coefficient K as a Function of
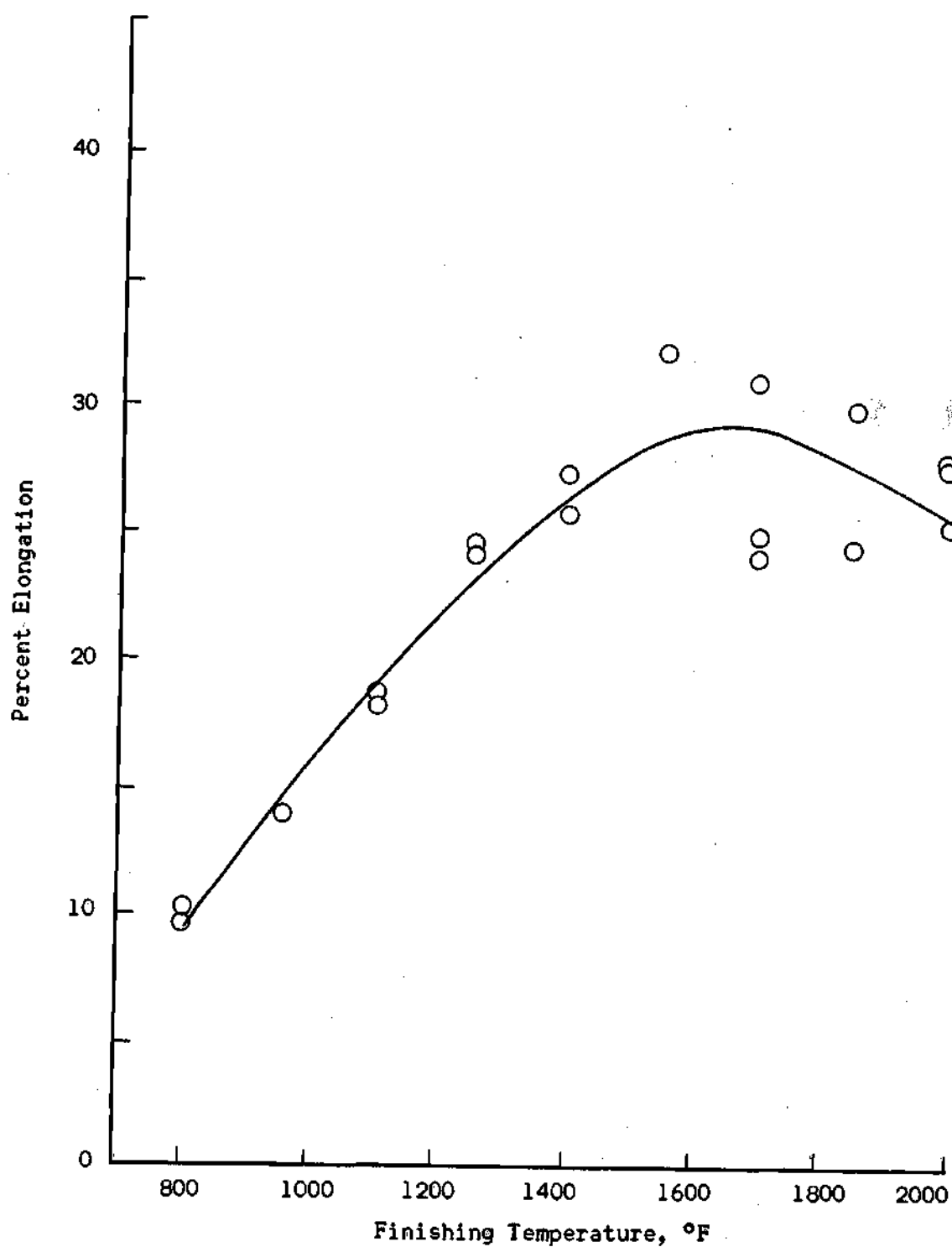Finishing Temperature: Cold Work -Hot
Work, Longitudinal Specimens.
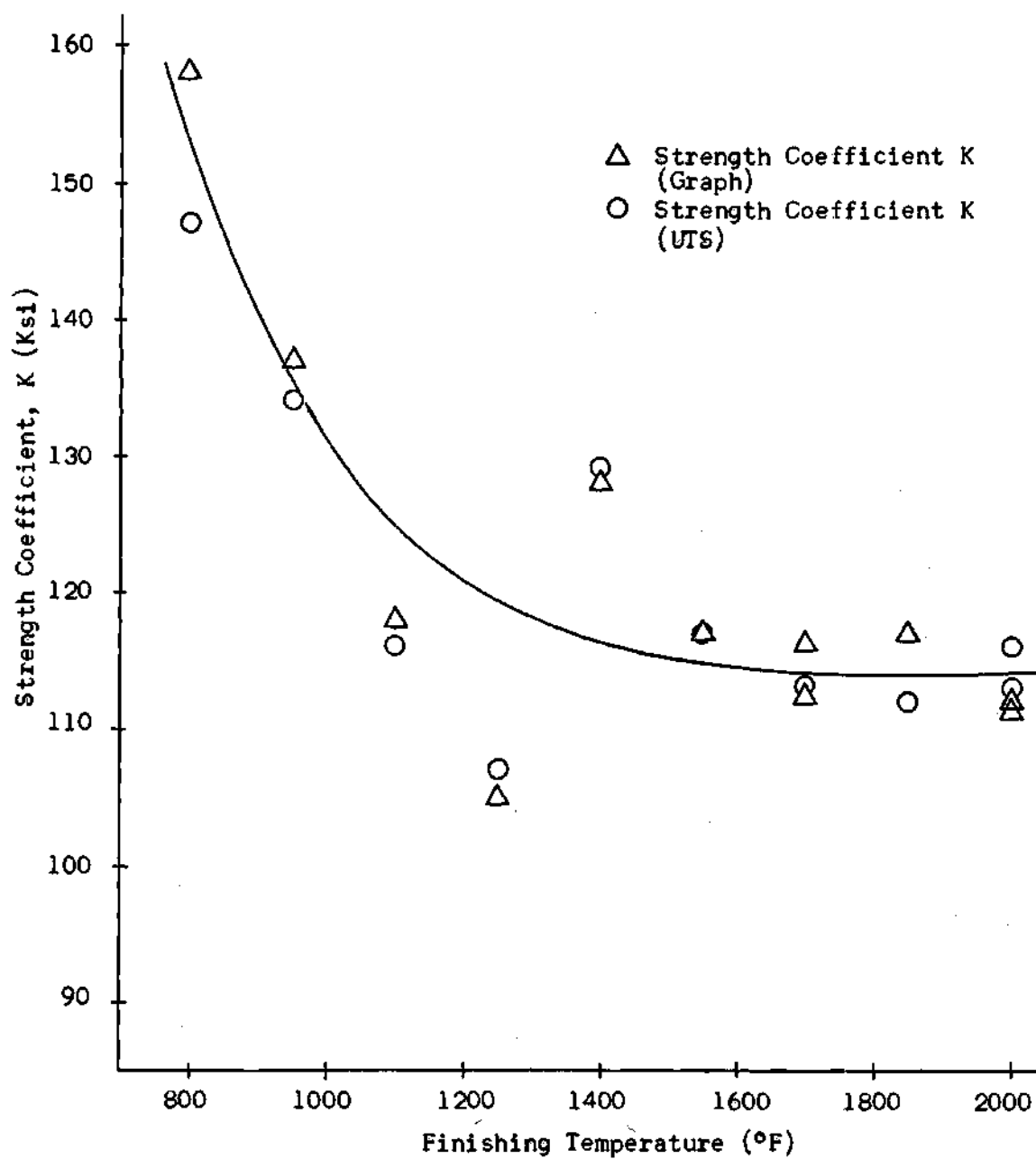
Figure 18.   Strength Coefficient K as a Function of
             Finishing Temperature: Cold Work -Hot
             Work, Transverse Specimens

Figure 19. Percent Elongation as a Function of Finishing
Temperature: Cold Work -Hot Work,
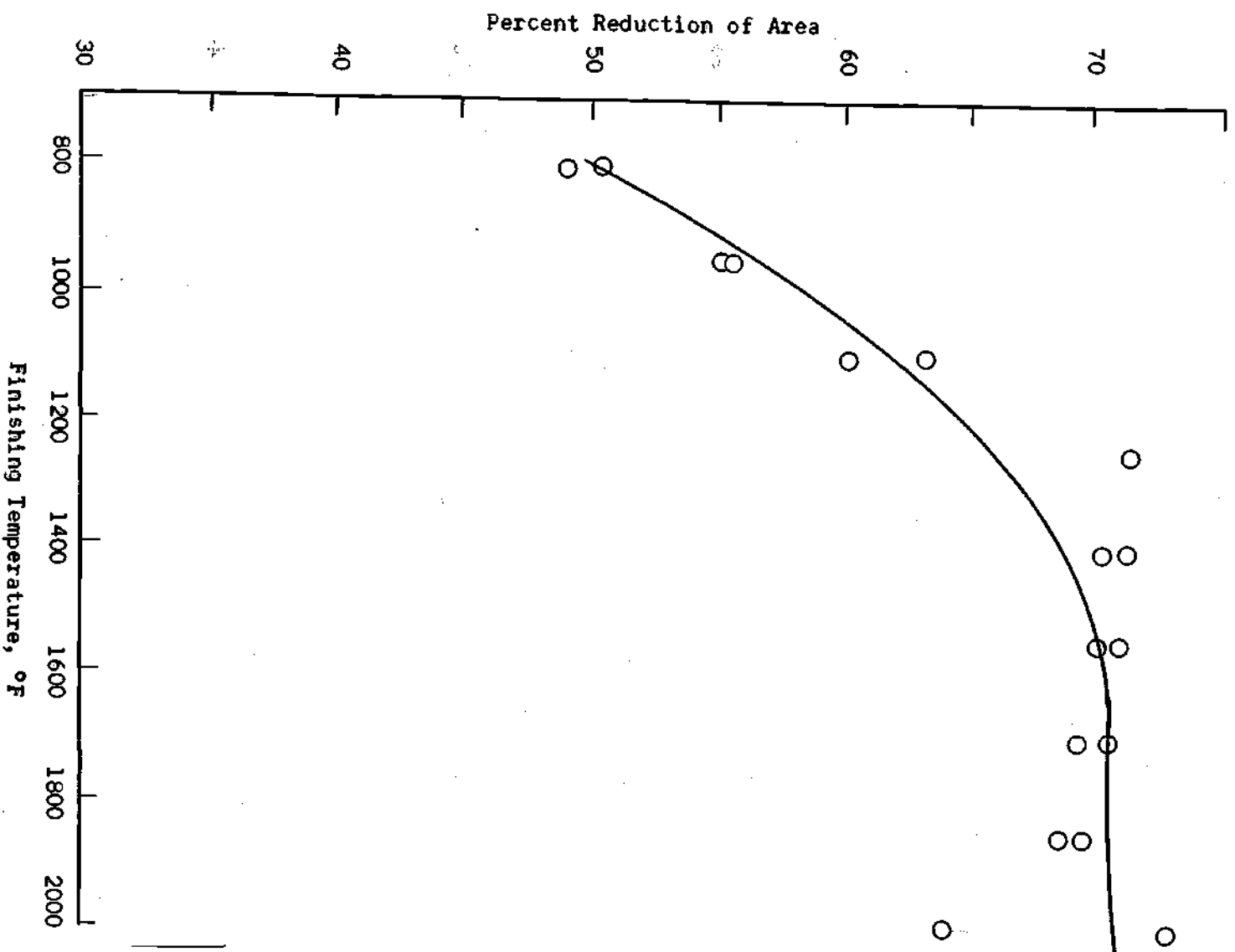Longitudinal Specimens.

Figure 20. Percent Reduction of Area as a Function of
Finishing Temperature: Cold Work - Hot
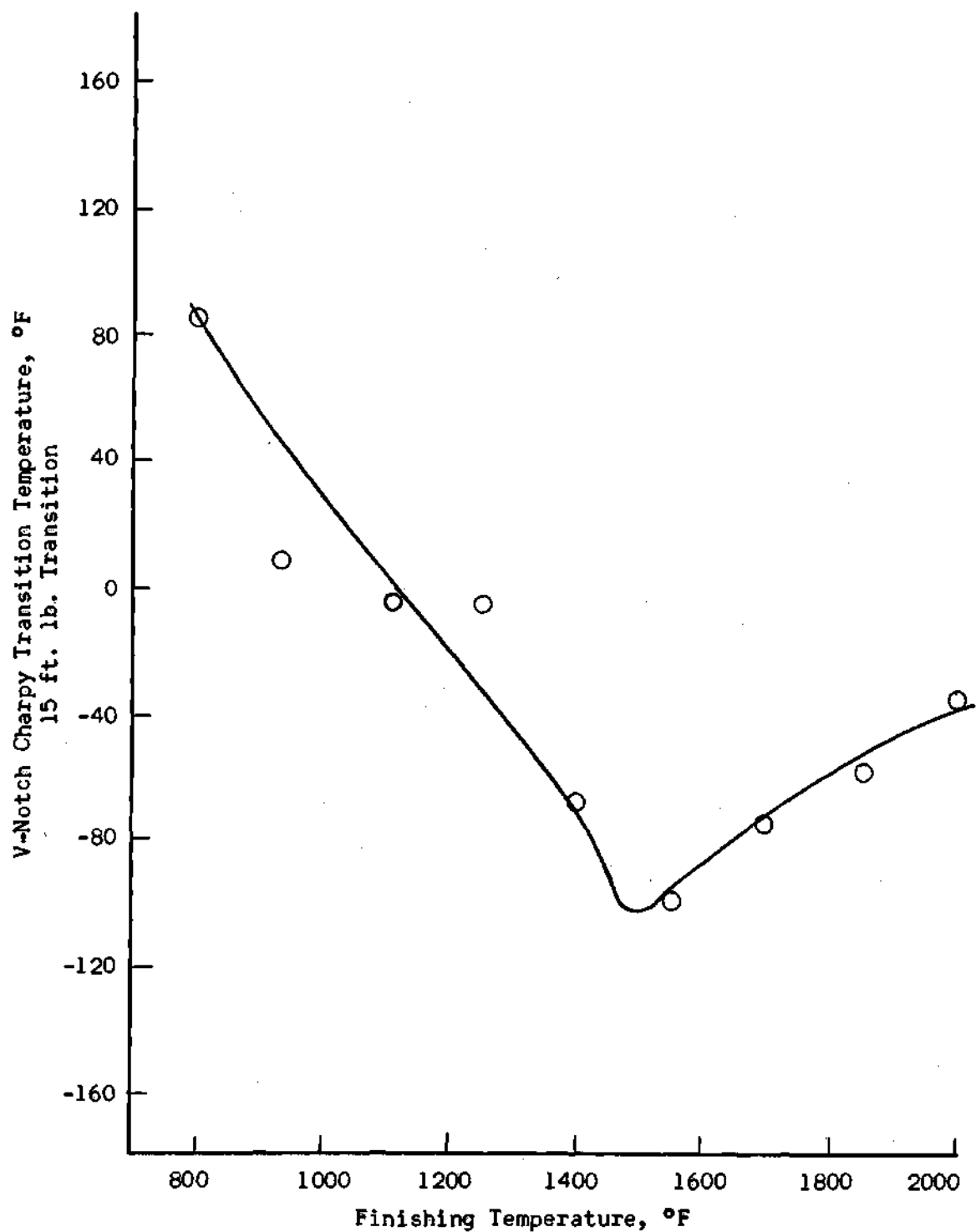Work, Longitudinal Specimens.

Figure 21.   V-Notch Charpy Transition Temperature as a
             Function of Finishing Temperature: Cold
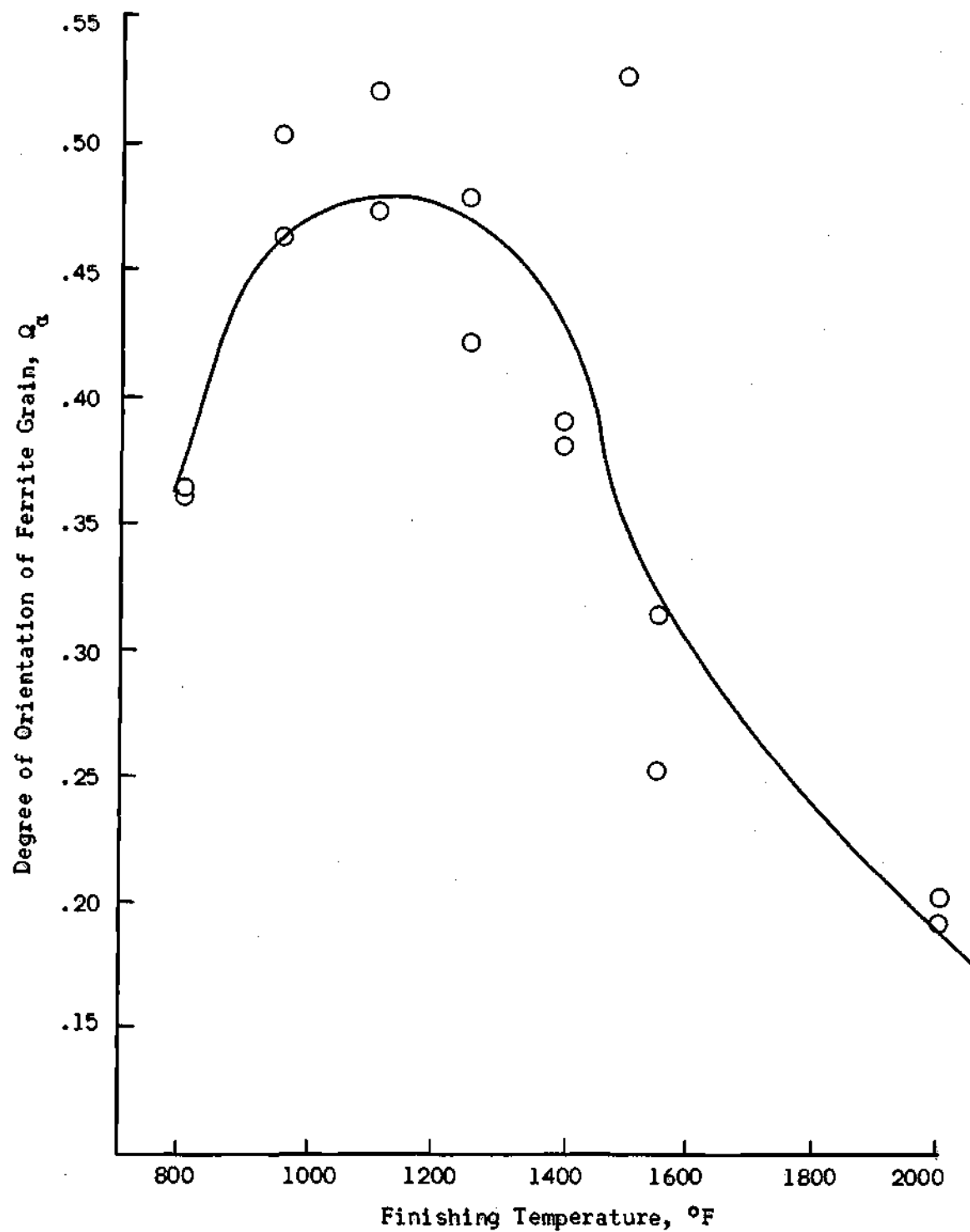   Work -Hot Work Specimens.

Figure 22.   Degree of Orientation of Ferrite Grain as a Function
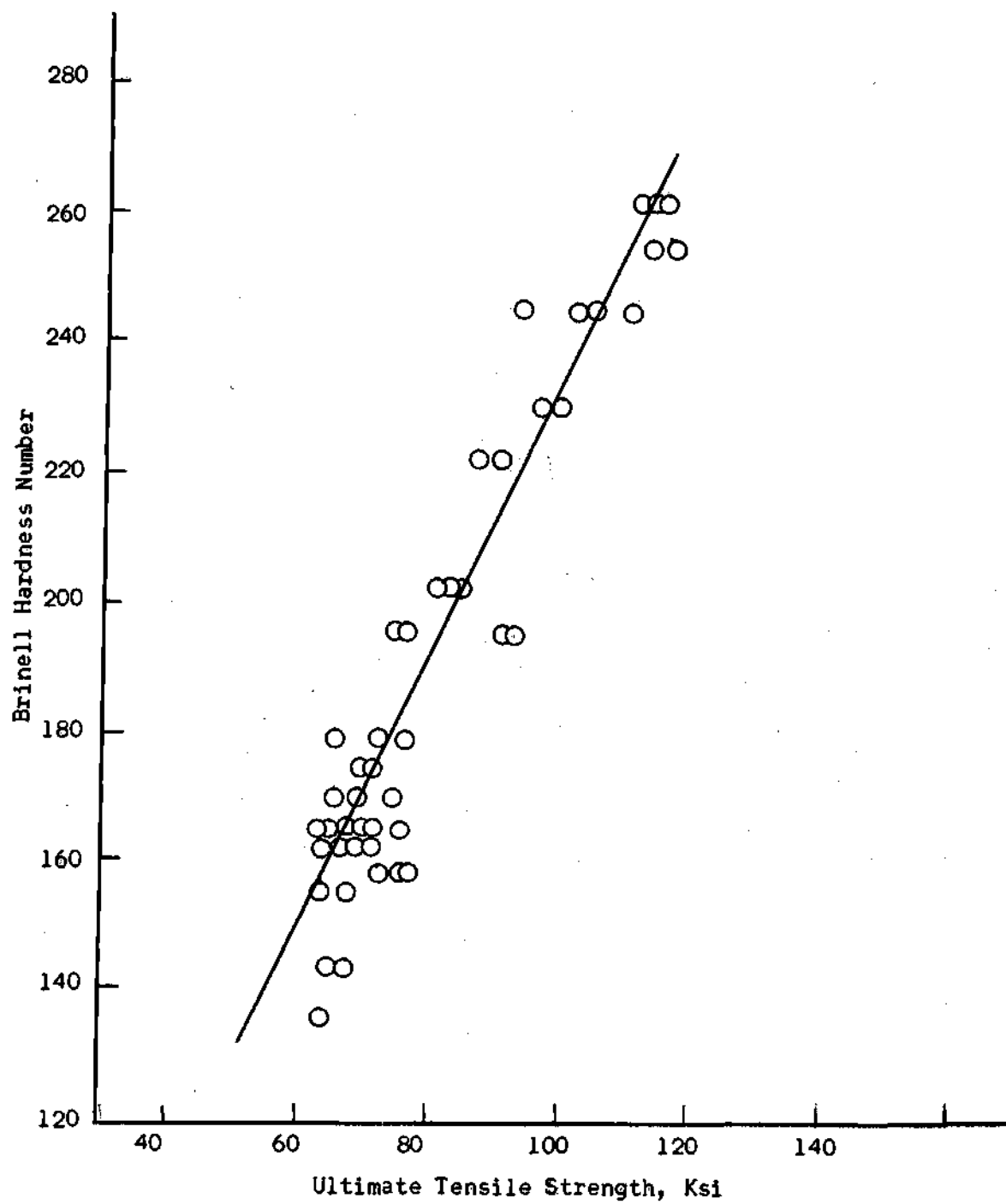of Finishing Temperature: Cold Work - Hot Work
Specimens.

Figure 23.   Brinell Hardness Number as a Function of
Ultimate Tensile Strength.

BIBLIOGRAPHY

1. Anonymous, "Composition, Properties, and Producers of High Strength Steels," <u>Metal Progress</u>, Vol. 92, pp. 87, 1965.

2. Hall, E. O., "The Deformation and Aging of Mild Steel," <u>Proceedings of the Physical Society</u>, Vol. B64, pp. 747, 1951.

3. Petch, N. J., "The Cleavage Strength of Polycrystals," <u>Journal of the Iron and Steel Institute</u>, Vol. 174, pp. 25, 1953.

4. Pickering, F. B., and T. Gladman, "Metallurgical Developments in Carbon Steels," <u>British Iron and Steel Research Association Report</u>, 81, pp. 9, 1963.

5. Burns, K. W., and F. B. Pickering, "Deformation and Fracture of Ferrite-Pearlite Structures," <u>Journal of the Iron and Steel Institute</u>, Vol. 205, pp. 899, 1967.

6. Allen, N. P., "Tensile and Impact Properties of High-Purity Iron-Carbon and Iron-Carbon-Manganese Alloys of Low Carbon Content," <u>Journal of the Iron and Steel Institute</u>, Vol. 174, pp. 108, 1953.

7. Heslop, J., and N. J. Petch, "The Stress to Move a Free Dislocation in Alpha Iron," <u>Philosophical Magazine</u>, Vol. 1, pp. 866, 1956.

8. Irvine, K. J., and F. B. Pickering, "Low Carbon Steels with Ferrite-Pearlite Structures," <u>Journal of the Iron and Steel Institute</u>, Vol. 201, pp. 944, 1963.

9. MacDonald, J. K., <u>Ship Structure Committee Report SSC-73</u>, November, 1953.

10. Banta, H. M., R. H. Frazier, and C. H. Lorig, "Some Metallurgical Aspects of Ship Steel Quality," <u>Welding Journal Research Supplement</u>, Vol. 30, pp. 795, 1951.

11. de Kazinczy, F., and W. A. Backofen, "Influence of Hot Rolling Conditions on Brittle Fracture in Steel Plates," <u>Trans. ASM.</u> Vol. 53, pp. 55, 1961

12. Mackenzie, I. M., "Niobium Treated Carbon Steels," <u>Journal of the West of Scotland Iron and Steel Institute</u>, Vol. 60, pp. 224, 1963.

13. Biggs, W. D., <u>Brittle Fracture of Steel</u>, MacDonald and Evans, London, 1960.

14. Petch, N. J., "The Ductile-Cleavage Transition in Alpha Iron," *Fracture*, John Wiley and Sons, New York, pp. 54, 1959.

15. Rinebolt, J. A., and W. J. Harris, Jr., "Comparison of the Effects of Alloying Elements on the Lower and Upper Transition Temperature in Pearlitic Steels," *Trans. ASM*. Vol. 44, pp. 225, 1952.

16. Low, J. R., Jr., and M. Gensamer, "Aging and Yield Point in Steel," *Trans. AIME*, Vol. 158, pp. 207, 1944.

17. Tipper, C. F., "Effect of Direction of Rolling, Direction of Straining, and Aging on the Mechanical Properties of a Mild-Steel Plate," *Journal of the Iron and Steel Institute*, Vol. 172, pp. 143, 1952.

18. Garofalo, F., and G. V. Smith, "Effect of Time and Temperature on Various Mechanical Properties During Strain Aging of Normalized Low Carbon Steels," *Trans. ASM*, Vol. 47, pp. 957, 1955.

19. Gladman, T., B. Holmes, and F. B. Pickering, "Work Hardening of Low Carbon Steels," *Journal of the Iron and Steel Institute*, Vol. 208, pp. 172, 1970.

20. Pickering, F. B., "Some Aspects of the Relationship Between Microstructure and Mechanical Properties," *Iron and Steel*, Vol. 38, pp. 110, 1965.

21. Jamieson, R. M., and J. W. Thomas, "Controlled Rolling of High Strength Skelp for the Manufacture of Large OD Pipe," *Iron and Steel Institution Publication* 104, pp. 167, 1967.

22. Duckworth, W. E., and J. D. Baird, "Mild Steels," *Journal of the Iron and Steel Institute*, Vol. 207, pp. 854, 1969.

23. Irvine, K. J., "Physical Metallurgy," *Journal of the Iron and Steel Institute*, Vol. 207, pp. 837, 1969.

24. Korchynsky, M., Graham Research Laboratories, Jones and Laughlin Steel Corporation, Pittsburgh, Pennsylvania, personal communication to Dr. W. R. Clough.

25. Kouwenhoven, H. J., "The Influence of Ferrite Grain Size and Volume Fraction of Pearlite on the Lower Yield Stress and Luders Strain of Carbon Steel," *Trans. ASM*, Vol. 62, pp. 437, 1969.

26. Morrison, W. B., "The Effect of Grain Size on the Stress-Strain Relationship in Low Carbon Steel," *Trans. ASM*, Vol. 59, pp. 824, 1966.

27. Irani, J. J., and D. J. Latham, "Application of Isoforming and Applied Treatments Low Alloy Steels," _Iron and Steel Institute Publication 114_, pp. 55, 1969.

28. Irani, J. J., "Isoforming - A Technique of Deformation During Isothermal Transformation to Pearlite," _Journal of the Iron and Steel Institute_, Vol. 206, pp. 363, 1968.

29. Koppenaal, T. J., "The Current Status of Thermomechanical Treatment in the Soviet Union," _Trans. ASM_, Vol. 62, pp. 24, 1968.

30. Ivanova, V. S., and L. K. Gordienko, _New Ways of Increasing the Strength of Metals_, Iron and Steel Institute Publication 109, 1968.

31. Yeo, R. B. G., A. G. Melville, P. E. Repas, and J. M. Gray, "Properties and Control of Hot Rolled Steel," _Journal of Metals_, Vol. 20, pp. 33, 1968.

32. Latham, D. J., "The Current Position of Thermomechanical Treatments Applied to Engineering and Tool Steels," _Journal of the Iron and Steel Institute_, Vol. 208, pp. 50, 1970.

33. Cryderman, R. L., A. P. Coldren, J. R. Bell, and J. D. Crozier, "Controlled-Cooled Structural Steels Modified with Columbium, Molybdenum, and Boron," _Trans. ASM_, Vol. 62, pp. 561, 1969.

34. Duckworth, W. E., "Metallurgy of Structural Steels: Present and Future Possibilities," _Iron and Steel Institute Publication 104_, pp. 61, 1967.

35. Underwood, E. E., _Quantitative Stereology_, Addison Wesley, Reading, Massachusetts, 1970.